Czech Technical University in Prague

Faculty of Nuclear Sciences and Physical Engineering

Department of Nuclear Chemistry

Radiolabeling of polymer drug delivery systems with ^{68}Ga and tracking of hydrogel formation in vivo

Značení polymerních nosičů léčiv pomocí ^{68}Ga a sledování tvorby hydrogelu in vivo

Bc. Kristýna Kroftová

Master's thesis

Prague 2022

České vysoké učení technické v Praze
Fakulta jaderná a fyzikálně inženýrská

Katedra jaderné chemie Akademický rok **2021/2022**

ZADÁNÍ DIPLOMOVÉ PRÁCE

Student:	**Bc. Kristýna Kroftová**
Studijní program:	Aplikace přírodních věd
Specializace:	Jaderná chemie
Název práce (česky):	Značení polymerních nosičů léčiv pomocí ^{68}Ga a sledování tvorby hydrogelu *in vivo*
Název práce (anglicky):	Radiolabeling of polymer drug delivery systems with ^{68}Ga and tracking of hydrogel formation *in vivo*

Pokyny pro vypracování:

1. Vypracování literární rešerše přípravy a vlastností biopolymerů s ohledem na použití v medicíně jako nosičů léčiv, metod značení pomocí ^{68}Ga a specifika *in vivo* experimentů.
2. Syntéza a charakterizace vybraných polymerů pro účely značení ^{68}Ga.
3. Značení a charakterizace polymerů ^{68}Ga a provedení stabilitních testů.
4. Sledování kinetiky tvorby hydrogelů *in vitro*.
5. *In vivo* experimenty se značenými polymery.
6. Sepsání práce

Doporučená literatura:

[1] NAHM, Daniel. Development of Biomaterial Inks for the Additive Manufacturing of Chemically Crosslinked Hydrogel Scaffolds: disertační práce. Julius-Maximilians-Universität Würzbur, Würtzburg, 2020.

[2] HAHN, Lukas, Matthias BEUDERT, Marcus GUTMANN, et al. From Thermogelling Hydrogels toward Functional Bioinks: Controlled Modification and Cytocompatible Crosslinking. *Macromolecular Bioscience* [online]. [cit. 2021-10-12]. ISSN 1616-5187. Dostupné z: doi:10.1002/mabi.202100122

[3] DAS, Sudeep, Surachet IMLIMTHAN, Anu J. AIRAKSINEN a Mirkka SARPARANTA. Radiolabeling of Theranostic Nanosystems. FONTANA, Flavia a

Hélder A. SANTOS, ed. *Bio-Nanomedicine for Cancer Therapy* [online]. Cham: Springer International Publishing, 2021, 2021-02-05, s. 49-76 [cit. 2021-10-12]. Advances in Experimental Medicine and Biology. ISBN 978-3-030-58173-2. Dostupné z: doi:10.1007/978-3-030-58174-9_3

[4] SARPARANTA, Mirkka, Dustin W. DEMOIN, Brendon E. COOK, Jason S. LEWIS a Brian M. ZEGLIS. Novel Positron-Emitting Radiopharmaceuticals. STRAUSS, H. William, Giuliano MARIANI, Duccio VOLTERRANI a Steven M. LARSON, ed. *Nuclear Oncology* [online]. Cham: Springer International Publishing, 2017, 2017-10-29, s. 129-171 [cit. 2021-10-12]. ISBN 978-3-319-26234-5. Dostupné z: doi:10.1007/978-3-319-26236-9_87

[5] LEWIS, Jason S., Albert D. WINDHORST a Brian M. ZEGLIS, ed. *Radiopharmaceutical Chemistry* [online]. Cham: Springer International Publishing, 2019 [cit. 2021-10-12]. ISBN 978-3-319-98946-4. Dostupné z: doi:10.1007/978-3-319-98947-1

Jméno a pracoviště vedoucího práce:
Ing. Kateřina Fialová, Katedra jaderné chemie, Fakulta jaderná a fyzikálně inženýrská

Jméno a pracoviště zastupujících vedoucí práce:
doc. Mirkka Sarparanta, Ph.D., Department of Chemistry, University of Helsinki
prof. Robert Luxenhofer, Ph.D., Department of Chemistry, University of Helsinki

Datum zadání diplomové práce: 20. 10. 2021

Termín odevzdání diplomové práce: 2. 5. 2022

Doba platnosti zadání je dva roky od data zadání.

.....
Garant oboru

prof. Ing. Jan John, CSc.

.....
Vedoucí katedry

prof. Ing. Igor Jex, DrSc.

.....
Děkan

ČESKÉ VYSOKÉ UČENÍ TECHNICKÉ V PRAZE
Fakulta jaderná a fyzikálně inženýrská
-1-

V Praze dne 20. října 2021

Affidavit

I hereby confirm that this thesis is the result of my own independent work. All sources and/or materials applied are listed and specified in the thesis. Furthermore, I confirm that this thesis has not yet been submitted as part of another examination process neither in an identical nor in a similar form.

In Prague, 2. 5. 2022 ……

Signature

Acknowledgements

First and foremost, I would like to thank my supervisors, Ing. Kateřina Fialová, prof. Mirkka Sarparanta and prof. Robert Luxenhofer for their support, ideas, advice, and guidance through each state of the process. Without their assistance this thesis would have never been accomplished.

I would also like to show gratitude to my consultant RNDr. Martin Vlk, Ph.D as well as to doc. RNDr. Ján Kozempel, Ph.D for their motivation, expertise and vision. Thank you for providing me with all the necessary facilities for research.

I must also thank my colleagues, doctoral students Alessia Centanni and Larissa Keßler for all their help, contribution and patience that made this thesis happen. I am thankful for their, tips, recommendations, and wisdom, which filled my knowledge gaps in several areas.

I would like to give special thanks to prof. Ing. Jan John, CSc. and doc. Ing. Mojmír Němec, Ph.D, who helped me organize my internship in Finland, where I got introduced to the topic of this thesis. I take this opportunity to also acknowledge all members of the Department of Nuclear Chemistry, especially Ing. Tomáš Prášek and Bc. Jan Král, for their help and reassurance.

I also wish to express my sincere thanks to Mgr. Miroslav Vetrík, Ph.D. and his team from the Institute of Macromolecular Chemistry, Academy of Sciences of the Czech Republic for the preparation and characterization of the DTPA-rituximab conjugate. Their collaboration was a valuable contribution that helped to form the direction of this thesis.

Getting through my master's thesis required more than the academic support and I have many people to thank. Most importantly, I would like to express my very profound gratitude to my mom, Ing. Andrea Reifová, my brother, Bc. Jan Krofta, my grandma, Marie Kroftová, and my uncle, Petr Krofta, for their love and support throughout my years of study and while I was working on this thesis. Big love and thank you goes to my partner and best friend Ondřej Zelenka, who travelled with me to Finland. Thank you for putting up with me and for all your unfailing love and encouragement. Finally, I want to thank all my friends. Thank you for always cheering me up and for being here for me.

Název práce:	Značení polymerních nosičů léčiv pomocí ^{68}Ga a sledování tvorby hydrogelu *in vivo*
Autorka:	Bc. Kristýna Kroftová
Obor:	Jaderná chemie
Druh práce:	Diplomová práce
Vedoucí práce:	Ing. Kateřina Fialová, Skupina radiofarmaceutické chemie, Katedra jaderné chemie, České vysoké učení technické v Praze
Vedení na partnerském pracovišti:	prof. Mirkka Sarparanta, Ph.D., Tracers in Molecular Imaging group, Department of Chemistry, University of Helsinki prof. Robert Luxenhofer, Ph.D., Polymers and Colloids Group, Department of Chemistry, University of Helsinki
Konzultant:	RNDr. Martin Vlk, Ph.D., Katedra jaderné chemie, České vysoké učení technické v Praze

Abstrakt:

Tato práce si kladla za cíl charakterizaci přípravy a vlastností biopolymerů na bázi poly(2-oxazolinu) vzhledem k jejich využití v nukleární medicíně ve formě nosičů léčiv značených Ga-68. V teoretické části byla popsána pozitronová emisní tomografie (PET), vysoce citlivá zobrazovací technika, díky které vzrostla poptávka po pozitronových radionuklidech. Z tohoto důvodu byl navržen systém s biodistribucí léčiv založený na Ga-68 značených hydrogelech, který by poskytl selektivní PET diagnostiku a mohl být snadno syntetizován pomocí Dielsovy-Alderovy reakce.

V experimentální části byl popsán proces radioaktivního značení pomocí Ga-68 DOTA-modifikovaného polymeru a konjugátu DTPA-rituximabu. Výtěžek experimentů příslušných makromolekul označených Ga-68 byl stanoven pomocí vhodné metody chromatografie na tenké vrstvě. Značení bylo prováděno za různých podmínek. Ke sledovaným parametrům patřilo pH reakční směsi, aktivita Ga-68 a také teplota a délka inkubace. Dále byla sledována koncentrace radioaktivně značené látky ve vzorku a typ a objem rozpouštědla. Byly nalezeny vhodné podmínky radioaktivního značení DOTA-polymeru i DTPA-rituximabu pomocí Ga-68 a byla testována jejich stabilita.

Klíčová slova:

Gallium-68, hydrogely, poly(2-oxazoline), Dielsova-Aldera reakce, protilátky, rituximab, DOTA, DTPA, biokompatibilita, biodistribuce, radiofarmaka, diagnostika, PET, TLC.

Title:	Radiolabeling of polymer drug delivery systems with ^{68}Ga and tracking of hydrogel formation *in vivo*
Author:	Bc. Kristýna Kroftová
Branch:	Nuclear Chemistry
Type of thesis:	Master's Thesis
Supervisor:	Ing. Kateřina Fialová, Radiopharmaceutical Group, Department of Nuclear Chemistry, Czech Technical University in Prague
Co-supervisors:	prof. Mirkka Sarparanta, Ph.D., Tracers in Molecular Imaging group, Department of Chemistry, University of Helsinki
	prof. Robert Luxenhofer, Ph.D., Polymers and Colloids Group, Department of Chemistry, University of Helsinki
Consultant:	RNDr. Martin Vlk, Ph.D., Radiopharmaceutical Group, Department of Nuclear Chemistry, Czech Technical University in Prague

Abstract:

This thesis aimed to introduce the preparation and properties of poly(2-oxazoline)-based biopolymers regarding their use in nuclear medicine as drug carriers with Ga-68. The theoretical part reviewed the positron emission tomography (PET), a highly sensitive imagining technique, which increased the demand for positron-emitting radionuclides. Therefore, a novel drug delivery system based on hydrogels radiolabeled with Ga-68 was described that would provide a selective PET diagnosis and could be easily prepared by the Diels-Alder reaction.

The experimental part evaluated a radiolabeling process of a DOTA-functionalized polymer and DTPA-rituximab conjugate with Ga-68. A thin-layer chromatography method was developed to determine radiolabeling yields of experiments with the respective macromolecules, which were performed under various conditions. Tested parameters included pH of the reaction mixture, Ga-68 activity, as well as the radiolabeling incubation temperature and time. Concentration of the radiolabeled compound in a sample, and type and volume of the solvent were examined. Ideal Ga-68 radiolabeling conditions for DOTA-functionalized polymer and DTPA-rituximab conjugate were found, and their stability was studied.

Key words:

Gallium-68, hydrogels, poly(2-oxazoline), Diels-Alder reaction, antibodies, rituximab, DOTA, DTPA, biocompatibility, biodistribution, radiopharmaceuticals, diagnosis, PET, TLC.

Abbreviations

ACN	acetonitrile
CT	computed tomography
DA	Diels-Alder
DCC	N,N'-dicyclohexyl carbodiimide
DOTA	1,4,7,10-tetraazacyclododecane-1,4,7,10-tetraacetic acid
DOTA-TOC	(DOTA-Phe^1-Tyr^3) octreotide
DTPA	diethylenetriaminepentaacetic acid
EDTA	ethylenediaminetetraacetic acid
EMA	European Medicines Agency
EtOH	ethanol
FDA	Food and Drug Administration
GPC	gel permeation chromatography
LCST	lower critical solution temperature
mAb	monoclonal antibodies
MALDI	matrix-assisted laser desorption/ionization
MeOH	methanol
MWCO	molecular weight cut-off
NHL	non-Hodgkin's lymphoma
NMR	nuclear magnetic resonance spectroscopy
NOTA	1,4,7-triazacyclononane-1,4,7-triacetic acid
OECD	Organisation for Economic Co-operation and Development
p-SCN-Bn-DTPA	l-(p-iso-thiocyanatobenzy1)-DTPA
PBS	phosphate-buffered saline
PEG	polyethylene glycol
PET	positron emission tomography
PEtOx	poly(2-ethyl-2-oxazoline)
PMeOx	poly(2-methyl-2-oxazoline)
POx	poly(2-oxazoline)
RIT	radioimmunotherapy
SSTR	somatostatin receptor

SÚKL	State Institute for Drug Control
THF	tetrahydrofuran
TLC	thin-layer chromatography
UCST	upper critical solution temperature

Symbols

A	activity [MBq]
a	chemical activity
i	variable
K_{ML}	^{68}Ga-chelator equilibrium constant
$\log K_{tr}$	decimal logarithm of transferrin binding constant
m_{polymer}	mass of a polymer in a sample [mg]
T	temperature [°C]
t	time [min, h]
u	standard deviation of the radiolabeling yield
u_{x_i}	uncertainty of the i^{th} variable
$V_{\mathrm{conjugate}}$	volume of DTPA-rituximab conjugate
V_{eluate}	volume of ^{68}Ga eluate [µl]
wt%	mass fraction (percentage by weight)
Y	radiolabeling yield
$\frac{\partial y}{\partial x_i}$	partial derivative of $y = f(x_i)$

Table of Contents

1 Introduction

Imagining techniques are the foundation of nuclear medicine. Positron emission tomography (PET) being one of them, is a useful tool in medical research and diagnosis [1]. Each year the demand for PET examinations increases. According to the OECD *Health Statistics 2021*, between the years 2006 and 2019 the number of performed PET examinations in the Czech Republic has increased nearly fourfold starting with 1.5 and rising to 5.5 PET exams per one thousand persons, the total number in 2019 being 58 407 exams. In addition, a significant growth has been recognized in all countries listed in the statistical overview [2], which suggests that a similar trend might occur in the upcoming years.

PET is based on the detection of a selected tissue with a radiolabeled compound. The biokinetics of this compound can bring valuable information about, for example, a tumor-related metabolism or an anomaly. Up to now, the most used radionuclide for such applications has been cyclotron produced ^{18}F in a form of ^{18}FDG [3,4]. Other short-lived radionuclides produced on a cyclotron include ^{11}C, ^{13}N and ^{15}O. An alternative production of positron emitting radionuclides is via a generator, which is the main source of ^{68}Ga. This isotope deserves a special attention for possible convenient coupling to biomolecules through a chelator. Because of the easy access to ^{68}Ga without the need of an on-site cyclotron, this principle could lead to a faster development and production of biocompatible radiopharmaceuticals for PET diagnosis [5].

Poly(2-oxazoline)s (POxs) are promising polymers for the synthesis of broad variety of biomaterials. They can be synthetized via living cationic ring opening polymerization, which allows a high control over their molecular weight and its distribution. By cautious selection of the amide side chains, it is possible to modify their physical and/or chemical properties. Even functional groups for crosslinking and the incorporation of biological stimuli can be considered. POxs have been reported to show excellent cytocompatibility. This advantage makes them suitable for a large variety of biomaterial applications. Moreover, the first successful *in vivo* studies of POx drug conjugate suggest a favorable introduction of these materials to the pharmaceutical world [6,7].

Tumor-specific targeting compounds are the central aim of imaging and therapy in modern oncology. In the past decade, POx-based polymers have gained attention for the development of targeted drug delivery system. A study [8] of biodistribution of radiolabeled POx polymer *in vivo* shows a low accumulation of the polymer in the reticuloendothelial system (liver and spleen), which would make POx a suitable candidate for applications in nuclear medicine. The first step to develop tumor targeting compound with POx carriers could be the synthesis of a defined POx polymer conjugated to a common chelator 1,4,7,10-tetraazacyclododecane-1,4,7,10-tetraacetic acid (DOTA). Aminocarboxylate macrocycle DOTA is the "gold standard" bifunctional ^{68}Ga chelator, mostly used in ^{68}Ga-DOTATOC for clinical somatostatin receptor imaging. Despite the high stability of the ^{68}Ga-DOTA complexes, DOTA has some drawbacks. Typically, the radiolabeling conditions for ^{68}Ga require elevated temperature and acidic pH, which can be unsuitable for many biomaterials including biopolymers [7,9]. Another approach could therefore be a POx polymer conjugated to diethylenetriaminepentaacetic acid (DTPA), which is more convenient for the possibility of radiolabeling with ^{68}Ga under milder conditions, i.e., at room temperature [10].

In this thesis the preparation and properties of biopolymers regarding their use in nuclear medicine as drug carriers were evaluated and radiolabeling methods with ^{68}Ga were described. A radiolabeling process of a biocompatible polymer conjugated to DOTA and monoclonal antibody conjugated to DTPA was studied. A thin-layer chromatography (TLC) method was developed to determine the radiolabeling yields of the experiments that were performed under various conditions. Tested parameters included pH of the reaction mixture, ^{68}Ga activity, as well as the incubation temperature and time. Furthermore, concentration of the compound in a sample was examined, including type, concentration and volume of the polymer solvent. Different techniques of ^{68}Ga elution were tried to achieve the highest possible volume activities for radiolabeling.

In summary, the goals of this thesis were to:

1. Complete literature research of the preparation and properties of biopolymers regarding their use in nuclear medicine as a drug carrier of ^{68}Ga.
2. Perform a synthesis and characterization of a DOTA-modified POx for the purposes of ^{68}Ga labeling.

3. Do radiolabeling experiments with the chelator modified polymer, as well as study radiolabeling conditions of DTPA conjugated to a monoclonal antibody prior to the compound coupling to the polymer chain.
4. Evaluate gained results.

2 Theoretical Background

2.1 Positron Emission Tomography

Since the early 1990s, the significance of PET has been increasing in the field of clinical practice. Compared to other radiodiagnostic methods, it can provide more detailed picture about the condition of a patient. PET is often combined with computed tomography (CT) to improve the spatial imaging of tissues during the examination. In PET, a specifically designed radiopharmaceutical enters the metabolic processes. Despite the following imagining being an *in vivo* detection, it is a non-invasive technique. PET scans are used to diagnose all kinds of disorders and anomalies, especially the metabolic activities of tumors and associated tissue hypoxia, proliferation, and cell expression [1,11,12].

PET is based on the introduction of a selected radiopharmaceutical labeled with a β^+ emitter into the patient's body. Important properties of an optimal PET tracer include easy production, a quick radiolabeling process and an efficient uptake of the tracer in the targeted tissue associated with a high specificity. In addition, a fast clearance from the non-targeted tissue, a high stability *in vivo*, and an absence of a host-immune response are also of a great significance. All this allows to proceed the PET imaging shortly after the radiotracer acquisition. Furthermore, while the patient's dose stays minimal, they are free to go home right after the examination is finished. For ideal diagnostics, the radiotracer should also demonstrate a high target-to-background ratios in the targeted tissue [13,14].

2.2 Gallium-68 and the Radiopharmaceutical Applications

The coordination chemistry of Ga is of great interest thanks to the potential use of gallium isotopes in radiopharmacy [15-18]. Gallium is a metal that belongs to the group 13 of the periodic table. Under physiological conditions it exists in the 3+ oxidation state, which is significant for its coordination chemistry in radiopharmaceutical applications. According to Lewis theory of acids and bases, it is classified as hard acid [19] and prefers to form chemical bonds with ionic and non-polarisable Lewis bases, such as nitrogen and oxygen atoms in carboxylate, phosphonate, or amino groups. The coordination chemistry of Ga is remarkably similar to Fe, not only for the charge, but also for the ionic radius (62 pm for Ga^{3+} and 65 pm

for Fe^{3+}) and the preference for the coordination number 6. This quality is important for the preparation of gallium radiopharmaceuticals, especially considering the biokinetics.

While transferrin, a plasma protein, has two sites of binding to iron, it also shows high affinities for Ga^{3+}. This protein is present in plasma in high concentrations of about $2.5 \cdot 10^{-3}$ M and the binding constant for Ga is significant $\log K_{\mathrm{tr}}\,(\mathrm{Ga}) = 20.3$ [20]. Therefore, when injecting Ga^{3+} in the form of low stability complex e.g., gallium citrate, over 90 % of this metal is transchelated by the transferrin [18].

In aqueous solution, the hydrated cation Ga^{3+} is stable enough only under ultra acidic conditions. Hydrolysis occurs at higher pH values and leads to the formation of an insoluble hydroxide $Ga(OH)_3$. To give an example, if a solution contains 37 MBq/ml of Ga, which is equal to the concentration of $4 \cdot 10^{-10}$ M of ^{68}Ga, $Ga(OH)_3$ precipitation is detected for pH above 3 if there are no stabilising ligands present in solution [18]. The described hydrolysis prevents simple and direct preparation of gallium radiopharmaceuticals in aqueous solutions with pH close to 7. The hydroxide $Ga(OH)_3$ acts as amphoteric compound and is soluble in acids. The solubility at basic pH is characterized by the following reaction

$$\mathrm{Ga(OH)_3\,(s) + \ OH^- \rightarrow Ga(OH)_4^-}, \qquad (1)$$

and occurs at pH greater than 7.4 [1]. To be used as a radiopharmaceutical, Ga must be thermodynamically stable in the compound at physiological pH values or kinetically inert during the detection period [18].

One of the advantages of Ga^{68} is that it is a positron emitter commonly produced by the $^{68}Ge/^{68}Ga$ radionuclide generator. The fast and simple recovery of ^{68}Ga via the elution with 0.1M HCl is done directly at the radiopharmaceutical department, which ensures that significant activity of the radionuclide is not lost during the transfer from a cyclotron, where majority of other positron emitting radionuclides are being produced. The decay scheme presented in Fig. 1 shows the radionuclide decay of ^{68}Ge, which is a parent radionuclide to ^{68}Ga. Germanium-68 decays via electron capture to ^{68}Ga with a half-life of 270.95 d. Formed ^{68}Ga decays with a half-life of 67.71 min to stable ^{68}Zn. The short half-life makes ^{68}Ga well compatible with the biokinetics and biological half-lives of several low, average, or macro-molecular weight biomolecules

i.e., peptides or antibodies. Gallium-68 is a positronic radionuclide with 89% positron branching that is accompanied by low photon emission (1077 keV, 3.22%) [16,18,21,22].

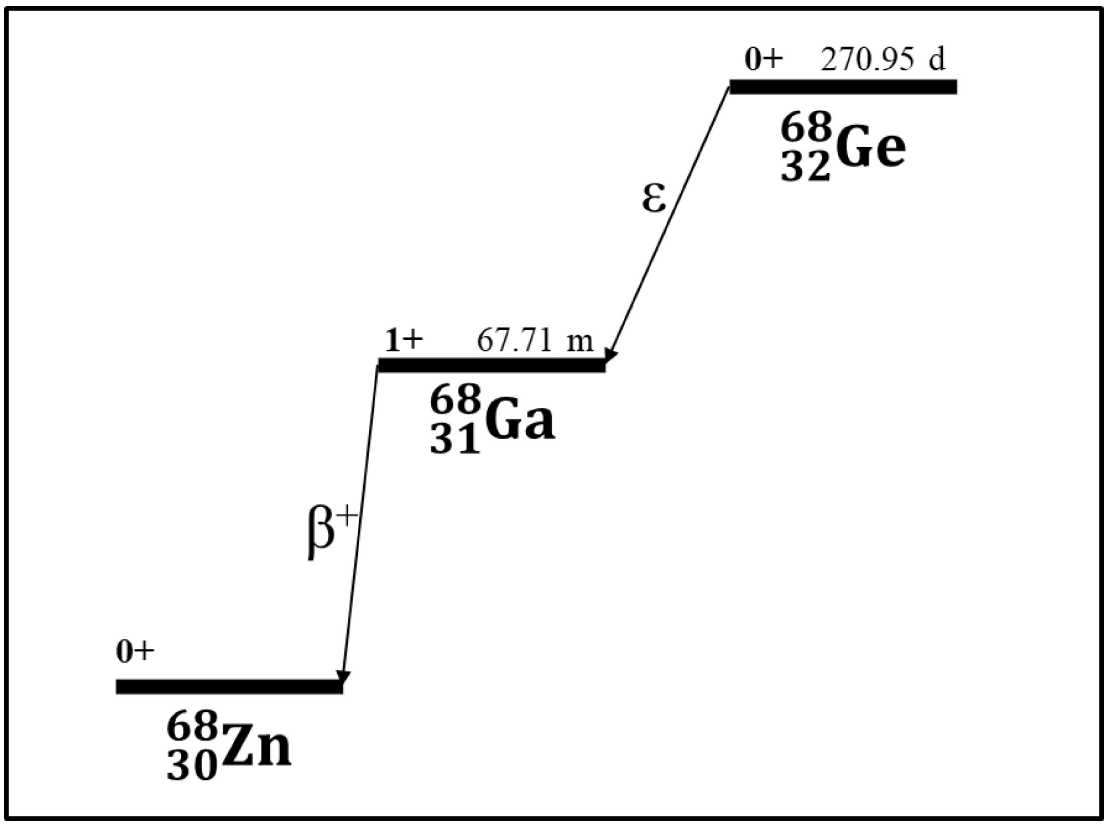

Fig. 1: The decay scheme of ^{68}Ga, including the parent ^{68}Ge [21].

Nowadays, due to additional purification steps, a satisfactory level of purity of ^{68}Ga obtained from a radionuclide generator is achieved. Yet, the cyclotron production remains an alternative source of the radionuclide through ^{68}Zn(p,n)^{68}Ga reaction. The reaction takes place on a zinc target and uses proton beam with the energy of about 13.2 MeV. The obtained ^{68}Ga is without any additional contaminants because of a highly specific separation system based on the ion-exchange chromatography [11,21].

The first ^{68}Ga radiopharmaceutical approved by the European Medicines Agency (EMA) for medical treatment in Europe became in 2016 ^{68}Ga-DOTA-TOC, commercially distributed as SomaKit TOC® [23]. In the Czech Republic, it was registered in the same year by the State Institute for Drug Control (SÚKL). The radiopharmaceutical is used for PET imaging of somatostatin receptor (SSTR) positive gastroenteropancreatic neuroendocrine tumors. This radiopharmaceutical combines

the radionuclide ^{68}Ga with the somatostatin analogue edotreotide for specific imaging of tumor cells expressing SSTRs. Such a targeting approach can be used for therapy planning of both localized and disseminated diseases [12].

2.2.1 TLC Quality Control of ^{68}Ga Radiopharmaceuticals

During the synthesis of ^{68}Ga radiopharmaceuticals two major chemical impurities are formed, they are ^{68}Ga-colloid and unbound ionic, or so called "free", $^{68}Ga^{3+}$. The amounts of each impurity in every radiopharmaceutical are strictly normalized according to the latest edition of European Pharmacopoeia [24], which describes methods for the separation and the detection of all expected impurities. Usually, more than one system is required to accomplish a complete quality control, with the simplest and fastest way being the TLC method. So far, no TLC method that would provide an effective separation of ^{68}Ga-colloid and a radiolabeled macromolecule (monoclonal antibodies or polymers) has been described, because they both remain on the base in all investigated systems [25]. To give an example, for the quality control of the widely used ^{68}Ga-DOTATOC (also known as SomaKit TOC or ^{68}Ga-edotreotide) two TLC methods are utilized. Both techniques are performed on a glass-fibre ITLC paper (e.g., Agilent ITLC SGI001) pre-cut to 1 cm x 12 cm strips, however, they differ from each other by the type of the mobile phase. The first method uses 77 g/l solution of ammonium acetate in water/methanol (1:1, by volume), while the second method requires aqueous solution of 0.1M sodium citrate (pH 5). Both plates are developed in a developing tank and scanned with a radiometric ITLC scanner. The first method results in chromatogram, where not complexed ^{68}Ga remains at the origin and ^{68}Ga-edotreotide migrates with the solvent front. Oppositely, the second method shows ^{68}Ga-edotreotide staying at the origin, while free ^{68}Ga moves with the front of the solvent. Such a separation provides an overall idea of the most probably occurring impurities [24].

2.2.2 Bifunctional Chelators

With the increasing number of PET centers and ^{68}Ga availability for molecular imaging, the search for new ligands for gallium has attracted the scientific attention. Particularly chelators have been of a great use to most targeted molecular imaging metal agents. Any potential chelator, which strongly complexes the metal, does either have to be a targeting molecule itself or is attached, either directly or through a linker,

to the targeting vector (e.g., a peptide or an antibody) [18]. The conjugation to the targeting molecule is achieved through a functional group (e.g., carboxylate or aryl) that is able to form a covalent bond to the biomolecule, creating a so called bioconjugate [18,26]. All chelators that are able to undergo this process are referred to as bifunctional chelators.

Tab. 1: Stability constants, $\log K_{ML}$ (2), for $^{68}Ga^{3+}$ polyaminocarboxylate complexes and respective pM values [27-29].

Chelator	$\log K_{ML}$	pM
EDTA	22.1	19.9
DTPA	24.3	22.8
DOTA	21.3	15.2
NOTA	31.0	26.4

Understandably, the requirements for the design of ^{68}Ga radiopharmaceuticals are closely related to $^{68}Ga^{3+}$ complex chemistry. To this day, many bifunctional chelators suitable for ^{68}Ga radiolabeling were proposed, developed, and conjugated to biomolecules [10,30-33]. For an ideal chelation, a rapid, quantitative, and stable coordination of $^{68}Ga^{3+}$ is essential. In addition, ^{68}Ga-chelator complexes have to provide satisfactory thermodynamic stability, which is characterized with a high equilibrium constant K_{ML} expressed as the following ratio between the chemical activity of the complexed cation, and the product of the activities of free cation and ligand in the solution [34]

$$K_{ML} = \frac{a_{ML}}{a_M \cdot a_L}, \tag{2}$$

where a_{ML} is the chemical activity of the complex, a_M is the chemical activity of free Ga^{3+}, and a_L is the chemical activity of the free complexing agent. Stability constants, $\log K_{ML}$, for complexes of the selected bifunctional chelators with $^{68}Ga^{3+}$ are summarized in Tab. 1. By themselves, the $\log K_{ML}$ values can indicate the relative affinity of the different chelators for a given metal, yet it can be difficult to compare stability constants for ligands in solutions of different pH. To overcome such difficulty, the pM values (pM = log[M]) must be considered to compare the actual quality of different chelators. The pM value reflects the influence of protonation, hydrolysis, ligand basicity and dilution. Increasing pM correlates with increasing stability [28].

Despite the hexadentate ligands, which correspond to the typical six-coordination sphere of Ga^{3+}, may seem like an obvious choice, many other studied ligands provide highly rigid and inert $^{68}Ga^{3+}$ complexes. The rigidity is achieved by selecting a chelator with both a "hard" donor atom with a high affinity for Ga^{3+}, which shows a remarkable charge density, and a correct geometry or topology. Therefore, chelators with conformations that undergo an octahedral Ga^{3+} binding also provide kinetically stable complexes [30]. The capability of a chelator to coordinate Ga^{3+} is based on its selectivity for Ga^{3+} over other metal ions, and the ability of other ions to compete with Ga^{3+} binding under physiological conditions. For example, for biological applications, ^{68}Ga-complexes must have a high resistance towards transchelation with transferrin, which is a protein that ensures the receptor-mediated transport of Fe into cells and shows significant affinity to ^{68}Ga due to the similarity of the coordination chemistry of trivalent Ga and Fe [18,20,27,30,31].

Theoretical ideal conditions for the ^{68}Ga radiolabeling in practice would be room temperature, near neutral pH (5, 6, 7 or 8) and low chelator concentration, all of which is convenient for radiolabeling biocompatible proteins or mAb that are vulnerable to unfolding or degradation at extreme pH and/or temperature. Chelators that would fulfil these requirements would allow a simple routine radiopharmaceutical preparation and a high benefit for the patients [30]. Yet, the formation of ^{68}Ga-chelator complex via radiolabeling is usually performed in acidic solutions with pH below 5. The reason is because hydrated Ga^{3+} species such as $[Ga(H_2O)_6]^{3+}$ prevail in solutions below pH 4. However, with pH increasing above ~4, the formation of poorly soluble hydrolyzed $Ga(OH)_3$, which competes with the radiolabeling, occurs significantly and remains until the pH exceeds 6.3, where soluble tetracoordinate $[Ga(OH)_4]^-$ predominates [16,17,30]. This chemistry is strongly temperature dependent and influenced by the presence of other metal ions and coordinating molecules in solution [35,36]. To accomplish an efficient $^{68}Ga^{3+}$ radiolabeling of chelate-peptide, chelate-polymer or chelate-mAb conjugates above pH 4, the chelation must effectively compete with ^{68}Ga-colloid formation, which is accomplished if the chelation rate is regulated by diffusion [18,27,30,31].

Based on their structural properties, bifunctional chelators suitable for trivalent $^{68}Ga^{3+}$ can be divided into two main categories, they are linear chain ligands and macrocyclic ligands [18]. For the labeling of peptides or, analogically, polymers, acyclic and cyclic

polyaminopolycarboxylic ligands such as DTPA, DOTA and 1,4,7-triazacyclononane-1,4,7-triacetic acid (NOTA) have been studied. These chelators are only a fraction of the wide variety of all developed chelating agents, nevertheless, they remain the core of the ^{68}Ga chelation chemistry. The benefit of them is that one of the carboxylic arms of polyaminopolycarboxylic ligands can be used for coupling to a functionalized peptide or polymer chain without compromising the stability of the formed metal complex. The three chelators are shown in Fig. 2 with formerly popular acyclic ethylenediaminetetraacetic acid (EDTA), which was used with ^{68}Ga only as a simple complexing agent [27,36].

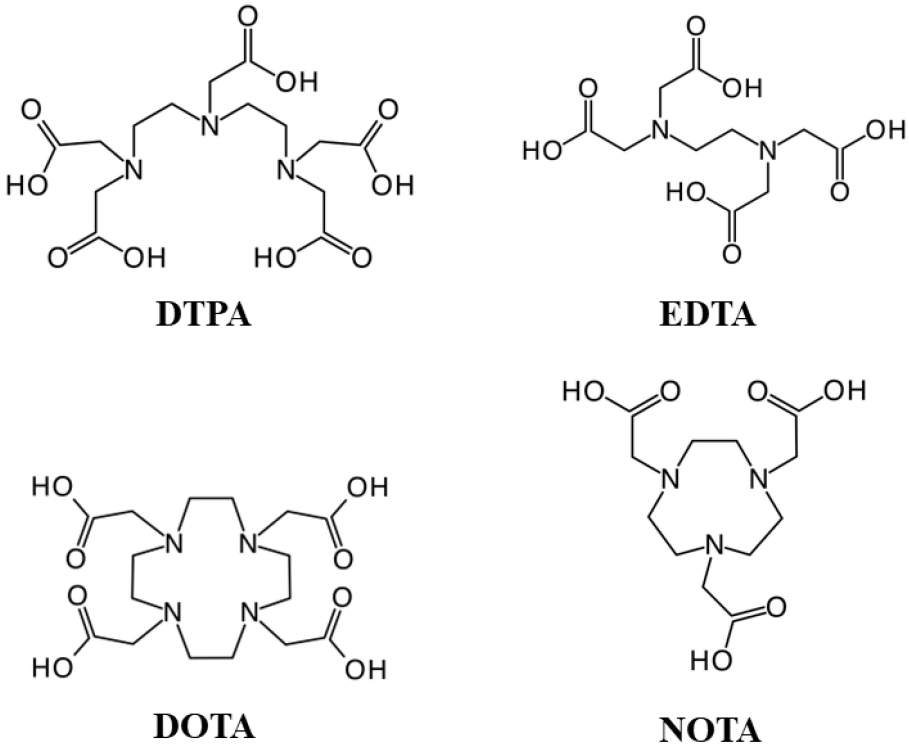

Fig. 2: Chosen acyclic and cyclic polyaminocarboxylic ligands.

2.2.2.1 Ethylenediaminetetraacetic Acid (EDTA)

The first clinically utilized ^{68}Ga chelator was acyclic EDTA (Fig. 2) in the late 1960s [31], a ligand well established for trivalent metal coordination chemistry. Aqueous EDTA solution was routinely employed for the elution of the first generation of ^{68}Ge/^{68}Ga radionuclide generators. The eluate with formed ^{68}Ga-EDTA complex (with stability constant $\log K_{ML} = 22.1$) was directly injected intravenously to the patients for perfusion monitoring of various organs, in particular, for the monitoring of brain activity [34].

2.2.2.2 Diethylenetriaminepentaacetic Acid (DTPA)

Among all radiopharmaceuticals, DTPA (Fig. 2) is one of the oldest, as well as one of the most often applied acyclic chelators. It can be radiolabeled with a variety of radiometal ions at room temperature within minutes [37], therefore DTPA can be utilized for radiolabeling of fragile compounds such as monoclonal antibodies and peptides [18]. So far, the clinical use of DTPA as a bifunctional chelator has been approved by both the EMA and SÚKL with ^{111}In as the SPECT radiopharmaceutical ^{111}In-DTPA-octreotide for specific imaging of the somatostatin receptors of neuroendocrine tumors. The DTPA conjugation to the peptide can be accomplished with a DTPA-dianhydride, which is also convenient for coupling to human insulin for insulin receptors imagining [28,31,37]. A study was performed, where a similar conjugation was utilized in order to couple DTPA with human insulin to imagine insulin receptors with ^{67}Ga [38]. The radiolabeling was carried out for 30 minutes in 0.1M phosphate buffer (pH 8) at room temperature. Following *in vitro* stability testing in saline and human serum showed no evidence of major release of complexed ^{67}Ga after 2 hours. Alternatively, for imagining of tumor-localizing monoclonal antibodies of leukemia cells, l-(p-iso-thiocyanatobenzy1)-DTPA (*p*-SCN-Bn-DTPA) was synthetized [39], conjugated to anti-CD45 monoclonal antibody, labeled with ^{68}Ga and incubated for 10 minutes at room temperature in 1M sodium acetate (pH 5). The following tests discovered very high stability after 4 hours [33]. Furthermore, a ^{68}Ga radiolabeling of a nontargeted *p*-SCN-Bn-DTPA complex was performed in 0.5M ammonium acetate buffer to accomplish higher yields over the competitive ionic impurities potentially present in ^{68}Ga eluate. Only a small effect on the DTPA complexation ability for ^{68}Ga was recognized, except in the presence of Fe^{3+}, however, the thousand times molar excess of other metal ions present in human serum (Cu, Ca, and Zn) showed a significant influence on the complex stability [10]. Nevertheless, the high ^{68}Ga-DTPA stability constant (2) $\log K_{ML} = 24.3$ still suggests a favorable formation of this complex compared to clinically used ^{68}Ga-DOTA chelation (Tab. 1) [27].

2.2.2.3 1,4,7,10-tetraazacyclododecane-1,4,7,10-tetraacetic Acid (DOTA)

Despite the fact that among other polyaminopolycarboxylic ligands (Tab. 1) chelators based on DOTA (Fig. 2) do not always provide complexes with $^{68}Ga^{3+}$ with the

superior stability, DOTA-like chelators are the most frequently used macrocyclic chelators for PET applications [27,31]. That is probably due to the commercial abundance of various activated DOTA derivatives for several possible conjugation reactions. DOTA was first synthetized back in 1976, however, it has not been used as a bifunctional chelator for the following 12 years. Nowadays, ^{68}Ga-DOTA-TOC is the only ^{68}Ga labeled radiopharmaceutical approved as an orphan drug. The relatively low stability constant of DOTA for $^{68}Ga^{3+}$ ($\log K_{ML}$ = 21.3), is caused by the small size of the ion, which therefore cannot fit perfectly in the cavity of DOTA. To achieve a rapid and efficient radiolabeling, temperature around 90° C and at least 5-minute incubation time is required [18,31]. Carboxylate donor functions in DOTA-based chelators have proved to be stable *in vivo* and are very well-suited for conjugation to biomaterials or biomolecules [28]. Accordingly, ^{68}Ga-DOTA complexes are often used for the radiolabeling of peptides, however, they are not appropriate for the labeling of monoclonal antibodies because of the lengthy complexation kinetics at room temperature [33].

2.2.2.4 1,4,7-triazacyclononane-1,4,7-triacetic Acid (NOTA)

NOTA (Fig. 2) is a hexadentate chelator, as well as one of the oldest and most successful chelators for applications with ^{68}Ga. It is mainly because of the smaller 1,4,7-triazacyclononane ring structure, where $^{68}Ga^{3+}$ fits better in the cavity, which is characterized with a high stability constant $\log K_{ML}$ = 31.0 (Tab. 1). Radiolabeling of NOTA can be performed within 15 – 60 minutes usually at elevated temperature (e.g., 95 °C, analogically to DOTA), however, high radiochemical yields are reported in some studies also for favorable room temperature. The formed complex provides an excellent *in vivo* stability [31,37]. Regardless of the fact that NOTA may be more stable and inert with ^{68}Ga compared to DOTA, it may not be the optimal choice for all functions (e.g., targeting of a specific peptide vector) due to the difference in charge and physical properties. The resulting neutral complex with NOTA may provide inferior *in vivo* properties with certain vectors compared to the charged complex formed with DOTA, which may, as well, illustrate the complicated chemistry that must be considered during radiopharmaceutical development [37].

2.3 Immuno-PET and Monoclonal Antibodies

The principle of radioimmunotherapy (RIT) is to selectively deliver specific radionuclide coupled to a monoclonal antibody (mAb) into tumors. The biological effects of the monoclonal antibody and of radiation are believed to be synergistic. One of the examples of positively radiosensitive cells are the lymphoma cells, where the CD20 antigen provides a superior RIT target because it is expressed with a high surface density in most lymphomas. While RIT results in depletion of both malignant and normal B cells, normal B cells demonstrate recovery within 6 months [40-42]. To this day, the most widely studied and clinically utilized radioconjugates are murine anti-CD20 mAbs, i.e., ^{131}I-tositumomab (BEXXAR®) or ^{90}Y-ibritumomab tiuxetan (ZEVALIN®), for the treatment of B cell non-Hodgkin's lymphoma (NHL). To achieve a more favorable biodistribution of the subsequently injected radiolabeled antibody, ^{90}Y-ibritumomab is combined with a preload of unlabeled rituximab (MabThera®, Rituxan®) [41,43]. Rituximab is a chimeric mouse anti-human CD20 monoclonal antibody [44]. The unlabeled rituximab prevents the radiolabeled antibody from binding to non-tumor sites such as normal B cells or spleen and most likely enables deeper penetration of the radionuclide into the tumor. In addition, rituximab provokes several mechanisms of tumor cell killing based on cytotoxicity, direct initiation of apoptosis and cell cycling blockade. Several studies have shown the effectiveness of RIT in patients with CD20 positive B cell NHL. Recently, the possibility of RIT with ^{90}Y-rituximab using a ^{90}Y-ibritumomab treatment schedule has been reported [40,42].

The development of RIT has resulted in the idea of immuno-PET technology [45]. Immuno-PET is a combination of the PET and a radiolabeled mAb, which causes a high sensitivity and high-resolution imaging with the specificity of a mAb. PET/CT is well suited for tracer quantification, while obtaining a precise anatomical information, which can later be used for diagnosis and treatment planning. Consequently, immuno-PET has the potential for imagining of molecular interactions, which can help with simulation of subsequent antibody-based therapy. An appropriate radionuclide for immuno-PET should possess a half-live that is compatible with the time needed for a mAb to achieve an optimal tumor-to-background ratios [40]. Gallium-68 could be a potential candidate because of its good availability, short half-live, relatively low production costs, and well-developed radiochemistry.

Furthermore, unlike majority of positron-emitters, ^{68}Ga is already routinely used for PET imaging. Another radionuclide tested for immune-PET was ^{89}Zr as ^{89}Zr-rituximab, where the whole-body distribution with and without a standard preload of unlabeled rituximab in patients with relapsed CD20 positive B cell lymphoma was studied [42]. Analogically, ^{68}Ga-DTPA-rituximab was tested in this thesis. The main benefit of such a complex is the potential reduced toxicity of the radiopharmaceutical, which is caused by ^{68}Zn, the decay product of ^{68}Ga. This stable nuclide is unlike ^{89}Y, the decay product of ^{89}Zr, biocompatible. In addition, its concentration *in vivo* is regulated by the zinc homeostasis, and it does not cumulate in undesirable tissue.

2.4 Poly(2-oxazoline)-based Biomaterials

POxs, also known as pseudo-polypeptides, form a versatile polymer class, which has been studied for various biomedical applications. Since the release of the first study that describes their *in vivo* biodistribution [8], POx-based materials have become a promising candidate for utilization in nuclear medicine, where their main function would be the formation of a hydrogel cover *in vivo* to protect the active ingredient of targeting radiopharmaceuticals. To achieve an optimal hydrogelation, a co-polymerization of POx and chemically similar poly(2-oxazine) has been used [46].

POxs are structural isomers of polypeptides that show specific properties, which are needed for the development of successful polymer-based pharmaceuticals. These properties include biocompatibility, solubility, thermoresponsivity, size variability and modulation of chemical functionality. POxs are synthetized via living cationic ring-opening polymerization of 2-oxazolines as is shown in Scheme 1. This reaction can be divided into three steps: the initiation, propagation, and termination, and provides polymers with a defined molecular weight distribution [47-49].

There are two main classes of hydrophilic biocompatible polymers, natural and synthetic, that are being tested for the construction of modern drug delivery systems. Overall, natural polymers (e.g., dextran, hyaluronic acid, or dextrin) often exhibit better enzymatic biodegradability than synthetic polymers (e.g. POxs or poly(2-oxazines)), however, synthetic polymers have several benefits. Their enzymatic biodegradability usually relies on an adjustable (partial) hydrolysis of the main chain, which results in a desirable and individually controlled rate of enzymatic

activity. Moreover, the synthetic polymers are easier to prepare in a required form, including complex structures. A routinely used synthesis provides negligible batch-to-batch differences and low risk of toxicity or undesirable physiological reaction [46,47].

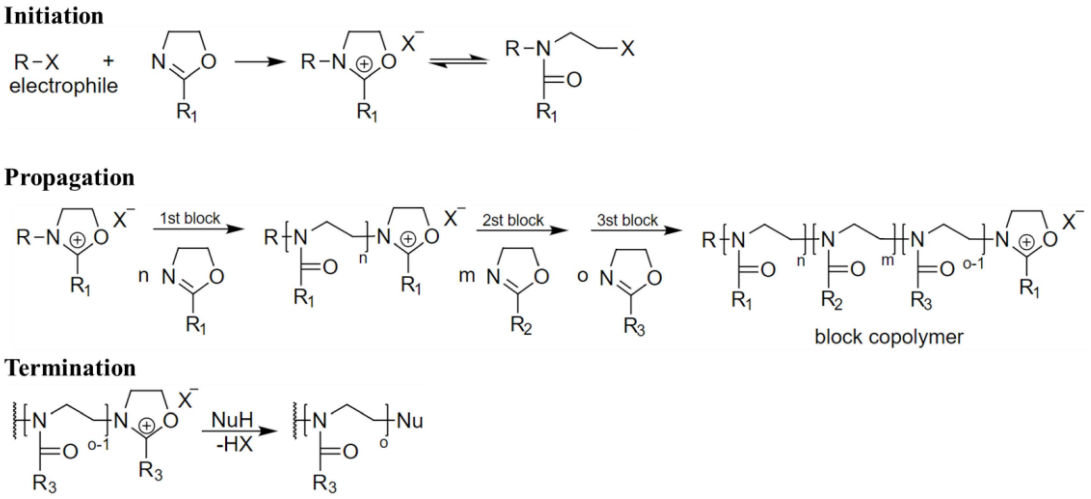

Scheme 1: Schematic representation of the initiation, propagation, and termination of the living cationic ring-opening polymerization of 2-oxazolines [48].

During the time, when POxs were first considered for medical applications, polyethylene glycol (PEG) became generally recognized as the popular polymer of choice. Aside from all qualities, it was mostly its convenient hydrophilicity that made PEG attractive enough to be commercially available. Modified PEG with different chelators was already tested several times to accomplish radiolabeling with varoius radionuclides including ^{68}Ga. For example, in [50], conjugation of radionuclide chelators via polyethylene glycol linkers was studied to prove a decreased nonspecific uptake of ^{68}Ga radiolabeled tracers.

POx-based polymers are often presented as PEG promising alternative. The biggest advantage of POxs over PEG lies in the enormous versality of the POx sidechains that allows this polymer to be modified for a large variety of biomaterial applications. The implementation of chelating agents such as DOTA to the side chains provides an efficient modification for potential ^{68}Ga PET radiopharmaceutical applications. This idea is utilized in the experimental part of this thesis. Moreover, aromatic side chain modification results in an increased hydrophobicity of the functionalized polymers. Based on this, a demanded solubility of POx *in vivo* can be achieved, which is applicable for a desired pharmacological biodistribution [47-48].

2.4.1 Physical Properties

Physical properties of POxs are tunable because of the endless possible variations of the monomer side chain, which is turned into the amidic side chains of the POx via the living cationic ring-opening polymerization. Depending on the length of the linear side chain, POx can either exist in an amorphous or in a semicrystalline form. In this work, a copolymer based on poly(2-methyl-2-oxazoline) (PMeOx) and poly(2-n-propyl-oxazine) was studied for ^{68}Ga radiopharmaceutical development. The preparation of such a radiopharmaceutical requires elevated temperature during incubation. For this reason, information about the expected structural properties and solubility under other than mild conditions is described in this chapter.

Studies regarding the thermal properties of POx discovered that, PMeOx to poly(2-n-propyl-oxazoline) remain amorphous and the formation of the first semicrystalline structure starts with poly(2-n-butyl-oxazoline). The melting point of POxs is around 150 °C, which is significantly above the necessary DOTA radiolabeling incubation temperature that does not exceed 95 °C. Moreover, the melting point is independent from the increasing length of the n-alkyl side chains, however it could be influenced by the branching of the sidechains, which makes the melting point even higher. For example, poly(2-isopropyl-2-oxazoline) and poly(2-isobutyl-2-oxazoline) are semi-crystalline with increased melting point around 210 °C compared to their linear analogues. In addition, using cyclic side chains can result in performance polymers with melting temperature values up to 306 °C.

In contrast to the melting temperature, it was found that the glass temperature is strongly dependent on the length of the n-alkyl side chains. There is a linear decrease from 80 °C affiliated with PMeOx to 24 °C for poly(2-n-butyl-oxazoline) [46,47,66]. Analogically to the glass temperature, solubility of POx is also strongly dependent on the chemical nature of the side chain. Shorter side chains, like methyl and ethyl, tend to be hydrophilic, however with four or more carbon atoms hydrophobicity occurs. Especially for medical use, the water solubility and hydrophilicity are an important quality. Apart from PMeOx, which should be even more hydrophilic than PEG, all water-soluble POxs show a lower critical solution temperature (LCST) behavior in aqueous solutions [46], which means that the polymers are dissolved better at low temperature by favorable hydration. With the increasing temperature, the entropy

driven dehydration results in a collapse of the hydrophobic polymer chains, which leads to worse solubility of the compound. Much less common is the opposite upper critical solution temperature (UCST) behavior in aqueous solutions, which means that polymers insoluble at low temperatures are soluble at elevated temperatures [52,53]. Copolymerization of hydrophilic and hydrophobic monomers can result in amphiphilic polymers, which are able to self-transition into superordinate structures like hydrogels or micelles. The formation of micelles can be also triggered as a result of thermoresponsiveness if the polymer concentration reaches the critical concentration. Such micelles have been widely studied for drug delivery applications [46,48].

An interesting choice of a solvent for POx is a water-ethanol mixture, which exhibits abnormal mixing properties because of the presence of hydration shells around the ethanol molecules [54-56]. According to literature [53], PMeOx and poly(2-ethyl-2-oxazoline) (PEtOx) are soluble in all water-ethanol solvent compositions at all investigated temperatures. Polymers with isopropyl and n-propyl side chains show LCST behavior in water and water rich ethanol solutions. Additional increase of the hydrophobicity of the side chain initiates the polymer insolubility to up to 35 wt% of ethanol content. After heating, a transitional behavior between insolubility and solubility in ethanol-water phase occurs. Thorough research of such an UCST transition shows that even a small hydrophobic side chain, or an intermediate aliphatic or aromatic side chain on a polymer could shield the hydrophilic amide groups in the polymer backbone.

Including ethanol as a solvent for DOTA-POx-based materials has many benefits, starting with increased solubility and more predictable behavior of the compound *in vitro*. A fraction of ethanol in the aqueous POx solvent mixture might prevent the polymer with LCST behavior from forming a hydrogel at elevated temperatures, which is significant for accomplishing an effective ^{68}Ga radiolabeling of DOTA-modified POx [18,31].

2.4.2 Biological Properties

It has been reported [47-49,53] that POxs demonstrate excellent biocompatibility. Nevertheless, such a general statement must be acknowledged critically as the current research approach does not usually go beyond *in vitro* cell cytotoxicity tests. Moreover, the attention is mainly focused on the hydrophilic PMeOx and PEtOx, for

which an excellent cyto- and hemocompatibility has been found. Novel POx biomaterials are often based on copolymers, which impacts the polymer composition, the molecular weight and the polymer ending groups. It also essentially alters the biological response. So far, many copolymers incorporating either PMeOx or PEtOx have been evaluated on their cytotoxicity and overall, no signs were found [57-61]. Even though testing the toxicity is an important aspect, understanding of the new biomaterials biodistribution mechanism is vital. *In vivo* radiolabeling studies in mice revealed a rapid clearance of POx-based homopolymers and copolymers from the bloodstream. [7,8] Additional studies show that only the polymers with a molecular weight below 20 kDa are excreted through kidneys [62], while biodegradability of polymers with high molecular weight can have diverse results. Moreover, the POx backbone is not easily degraded. Up to this date, no general biological degradation pathways were found. However, studies suggest degradation via enzymes or reactive oxygen [63].

2.4.3 Hydrolysis of Poly(2-oxazoline)

The first step to achieve a desirable degree of hydrolysis, in order to obtain an intended DOTA-polymer functionalization, is to perform a partial hydrolysis a POx-based polymer. In the experimental part of this thesis a copolymer (methyl-methyloxazoline$_{100}$-*b*-npropyloxazine$_{100}$-pipecolic acid polymer), synthetized and characterized by Robert Luxenhofer et al. [46] was used (Fig. 3). The partial hydrolysis of a selected amide bond in the POx part of the polymer chain was carried out under acidic conditions (Scheme 2).

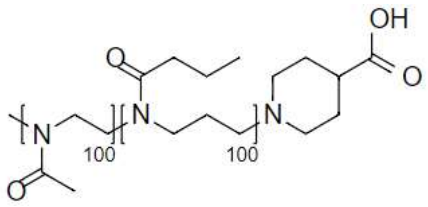

Fig. 3: Structure of POx-based copolymer used for DOTA functionalization.

Generally, the hydrolysis of POx is a rather slow process, which can take from several hours to days [64]. Despite the relatively high chemical stability of the POx backbone chain [65], POx amide side chains are easily cleaved off via hydrolysis in concentrated acid or base. This mechanism is not applicable under physiological conditions [7,65], where no significant hydrolysis was observed even in simulated intestine fluid [61].

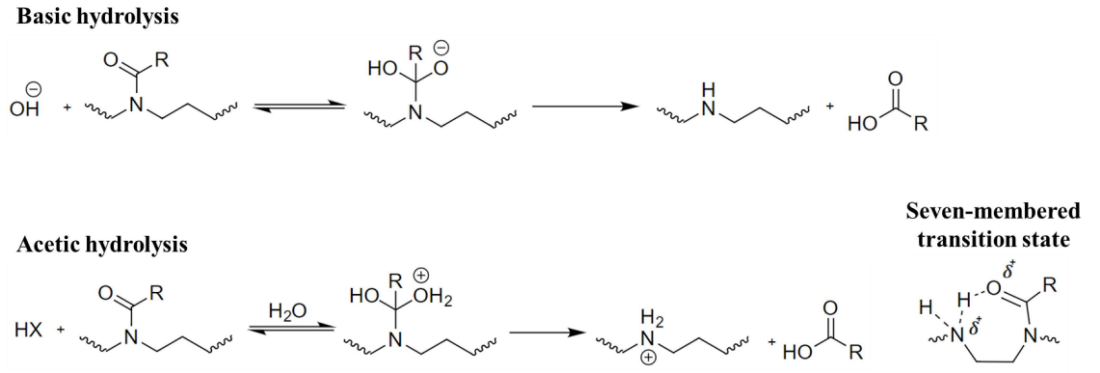

Scheme 2: The mechanism of the POx hydrolysis under basic and acidic conditions, with the seven-membered transition state responsible for the accelerated hydrolysis under acidic conditions [46].

Under basic conditions, hydrolysis is proceeded by OH^- nucleophile attacking the carbonyl group, as demonstrated in Scheme 2. It results in the intermediate product deprotonation and the respective carboxylic acid elimination from the polymer. This ultimate step is practically irreversible. The reaction follows second order kinetics. In some cases, also a backbone degradation under the basic hydrolysis conditions can occur [66]. Earlier reports might have overlooked this phenomenon because of the challenging analysis via gel permeation chromatography (GPC), which is caused by strong polymer-column interactions. The hydrolysis reaction process is much faster under acidic conditions [67]. This reaction is usually performed in a large excess of HCl, where it follows a pseudo-first order kinetics as can be seen in Scheme 2. The amide is activated by protonation of the carboxyl oxygen that enables the attack of water, which also determines the reaction rate. The outcome of the former intermediate product dissociation is a secondary amine and a carboxylic acid [46,68]. For low to medium conversions, a previous detailed evaluation [68] of the PMeOx and PEtOx acidic hydrolysis describes a linear dependence of the hydrolysis degree on the reaction time. For hydrolysis degrees that are about 60 % and higher, the polymer solubility decreases, which results in a partial precipitation and a slight deviation from the linear dependency. The hydrolysis kinetics appears to be independent of the total amide concentration. Furthermore, the molecular weight has also apparently no considerable influence on the reaction kinetics, although, in direct comparison, PMeOx hydrolyses more rapidly than PEtOx. This might be a result of the reduced steric hindrance combined with the increased hydrophilicity of PEtOx. On the other

hand, a study shows a strong dependence of the reaction kinetics on the reaction temperature [61].

Under acidic conditions a sudden formation of an intermolecular seven-membered ring may alter the reaction (Scheme 2). If an already hydrolyzed group is located next to an amide the probability that a neighboring amide will undergo hydrolysis is increased [61], which might result in the formation of hydrolyzed compartments within the polymer backbone. An acceleration of the hydrolysis speed in the first few minutes of the reaction is the indicator of the described mechanism [46].

Tailoring the hydrolysis degree is possible by using predefined hydrolysis kinetics and reaction time, which results in the synthesis of partially hydrolyzed POx with a defined amine content [61]. Utilizing the dependence of the hydrolysis kinetics on 2-alkyl-2-oxazoline side chain allows a selective and possibly partial hydrolysis of POx block-copolymers, which has been successfully employed as a starting point for polymer analogue modification. During such a process, secondary amines are formed in the polymer backbone (Scheme 2) by cleaving the amide bonds in the side chains. This allows further polymer-analogue functionalization with furan using a dicyclohexylcarbodiimide (DCC) supported coupling of 3-(2-furyl)propionic acid (Scheme 3) , followed by a Diels-Alder (DA) reaction between DOTA- maleimide and obtained furan group. This approach was used and described in the experimental part of this thesis for DOTA bifunctional chelator implementation to the polymer [46,69].

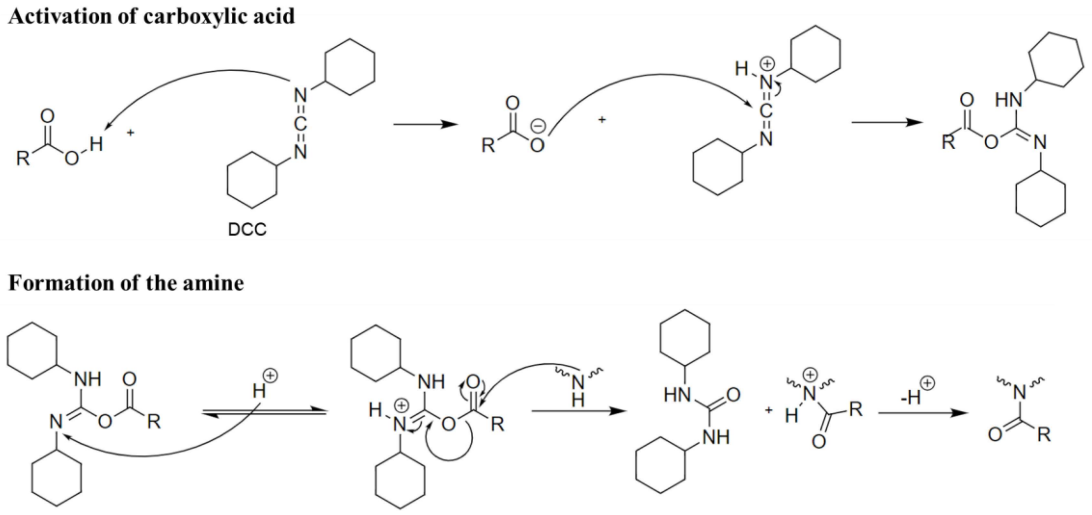

Scheme 3: Furan functionalization of POx chain using a DCC supported coupling of 3-(2-furyl)propionic acid.

2.4.4 Diels-Alder Chemistry

The approach to develop a tumor-targeting devices for PET imagining with POx carriers is a defined synthesis of POx polymers conjugated to DOTA, a widely used chelator for applications with ^{68}Ga [7,18]. Using click chemistry reaction without metal catalysators such as Cu, which would fill the cavity of DOTA during the synthesis, has many benefits. Click reactions have already been used in several publications for the synthesis of hydrogels with the focus on biomedical applications [70,71-75]. Particularly the DA reaction has several advantages for DOTA-POx conjugation, starting with the rapid and efficient chemistry proceeded under mild conditions without the requirement of a possibly toxic trigger [70,76-78].

So far, for the preparation of all POx-based hydrogels, modified polymer analogue of partially hydrolysed PMeOx has been used [72,79-82]. The functional groups for the crosslinking of the polymers were brought together by an amine acid coupling. Among other techniques, the covalent crosslinking was achieved by thermally reversible DA reaction of furan and maleimide, which is a click chemistry cycloaddition reaction that requires no catalyst or external trigger except of a temperature gradient [77]. The DA reaction offers foreseeable stereoselectivity, which is highly efficient. These qualities make DA chemistry a powerful tool among organic synthesis [83]. Moreover, the DA reaction is described as bioorthogonal, which means that it can be managed in living systems without disturbing their biological processes [84-87].

In the DA reaction a diene and an alkene, or so-called dienophile, undergo a [4+2] pericyclic reaction, during which six π-electrons are rearranged. This results into two new covalent carbon-carbon bonds establishment and a following six-membered ring formation. The DA reaction is concerted or proceeded in a single step with no intermediated products [88,89]. The most elemental example of DA reaction illustrated in Scheme 4 is a reaction between 1,3-butadiene and ethylene, which interestingly occurs only under elevated temperature and pressure. The reaction kinetics depends significantly on the position of electrons in the educts. A favourable reaction can be accomplished by using electron rich dienes and electron poor dienophiles [77]. This requirement is met by efficiently pairing furan with maleimide, which was utilized in the experimental part of this thesis [71]. The electron donating capabilities of the oxygen atom make furan a rather electron rich heterocyclic compound [90], while the

C=C double bond of maleimide is quite electron poor because of the electron withdrawing effect of the carbonyl groups. This makes maleimides very suggestible for pericyclic reactions [46]. In addition, the reaction is perfectly stereoselective and stereospecific, so a prediction of the formed stereoisomer can be described according to Woodward-Hoffmann rules [91]. An important aspect of certain diene and dienophile pairs, including furan and maleimide, is the reversed DA reaction, which occurs at elevated temperatures (Scheme 4) [91,92]. Although this process has no potential biological application, it is important to keep it in mind during preparation of DA reaction-based furan-maleimide materials.

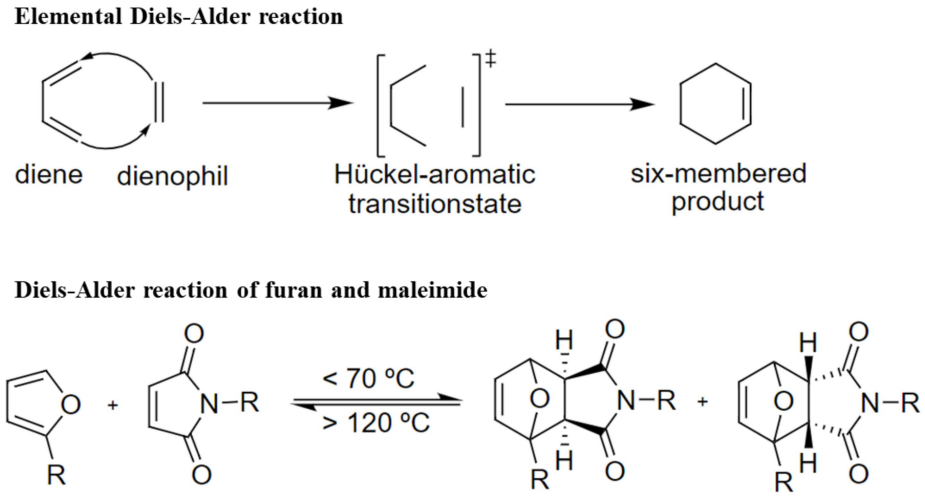

Scheme 4: Mechanism of the Diels-Alder reaction with an example of a reaction between furan and maleimide [46].

A few qualities make the DA reaction of furan and maleimide a suitable candidate for the synthesis of biomaterials. For instance, a variety of furan and maleimide derivatives are available commercially or easily synthesized, e.g., carboxylic acid derivatives of furan such as 3-(2-furyl)propionic acid [72]. In case of maleimides, carboxylic acid derivatives can be synthesized by conversion of maleic acid with amino acids [93]. The DA reaction between furan and maleimide can proceed swiftly in either aqueous solutions or without any solvent or dispersant [72,74,94-96]. The absence of any external stimuli means that no toxic solvents or chemical triggers are required, which makes purification step nearly unnecessary. Interestingly, due to a hydrophobic effect, the reaction proceeds faster in water-based solutions than in organic solvents [92]. To this day, the DA chemistry has been used for synthesis of materials for several biomedical applications [77,87,91,97,98]. Moreover, the mild DA

reaction, during which an antibody bioactivity is preserved, can be used for the bioconjugation of antibodies to polymeric nanoparticles for drug delivery applications [99]. A study was reported [7], where well defined conjugation of water-soluble POx with DOTA at the chain end was used for radiolabeling with ^{111}In to investigate the *in vivo* distribution and excretion of the compound in mice. It was found that the hydrophilic POx does not accumulate in tissues and is rapidly cleared from the blood pool, predominantly by glomerular filtration in the kidneys, while a small fraction is excreted via the hepatobiliary tract. Only negligible amount of POx is taken up by the reticuloendothelial system. Since additional functionalities for targeting can readily be conjugated to POx via functional monomer units, more compounds could be prepared for applications as radionuclide carriers for nuclear medicine.

2.4.5 Synthesis of a DOTA-modified Poly(2-oxazoline)-based Polymer

The first step to prepare a POx-based drug delivery system for a specific PET imaging with ^{68}Ga, where *in vivo* formation of protective hydrogel would occur, is a partial acidic hydrolysis of a PMeOx and poly(2-n-propyl-oxazine)-based copolymer (methyl-methyloxazoline$_{100}$-*b*-npropyloxazine$_{100}$-pipecolic acid polymer). The reaction results in a polymer main chain hydrolysis to a desired degree. This step should then be followed by an amine-acid coupling with 3-(2-furyl)propionic acid supported by DCC to ensure the furan functionalization of the main chain. After that, the click chemistry DA reaction between the furan functionalized polymer and DOTA-maleimide can be proceed under mild conditions (37 °C), which results in a DOTA-modified polymer preparation. The described process is demonstrated in Scheme 5.

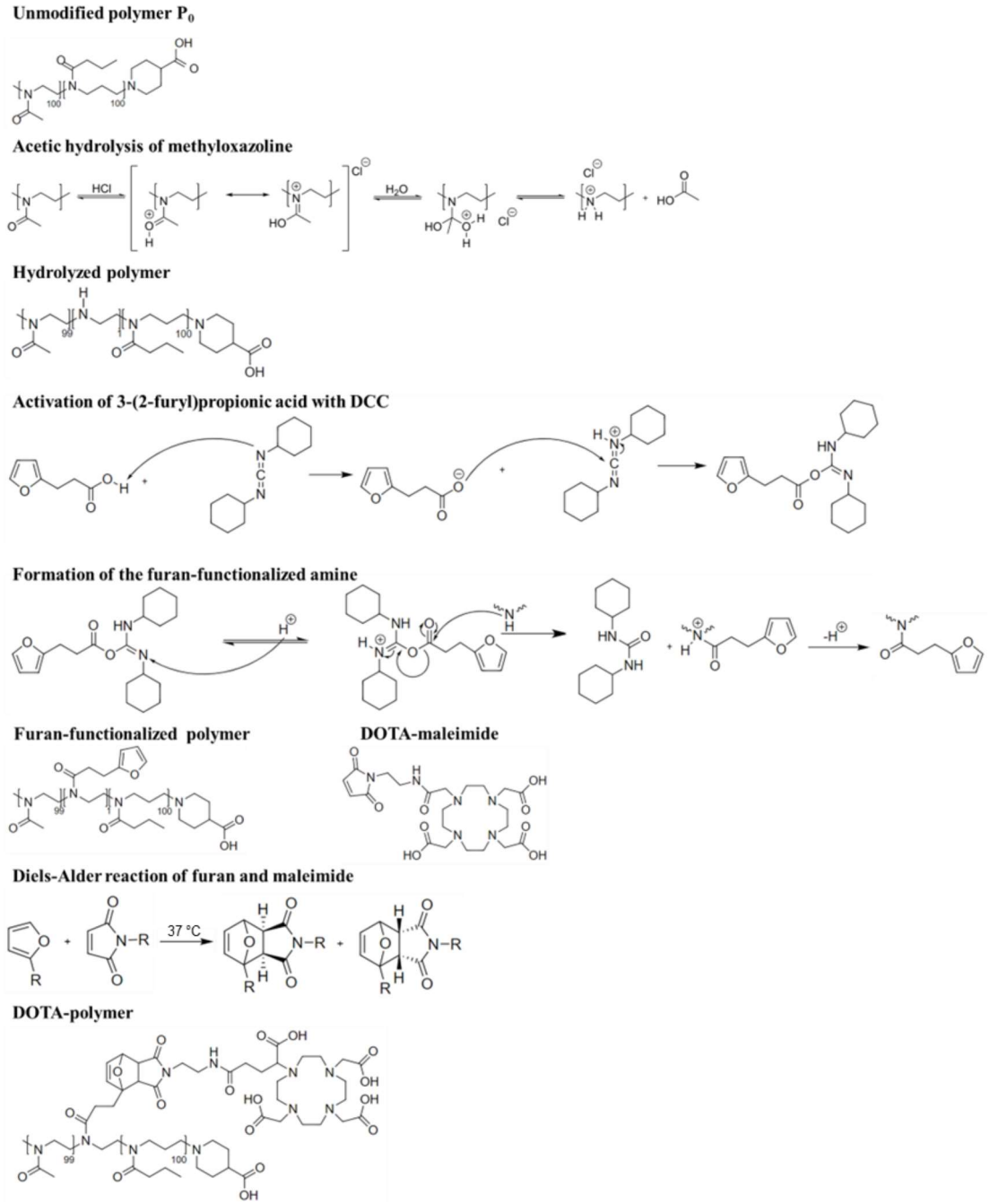

Scheme 5: Preparation of POx-based DOTA-modified polymer.

2.4.6 Hydrogels

The topic of POx based hydrogels was first presented in the early 1990's [72,79-82]. Hydrogels are polymeric water-swollen three-dimensional networks that are cross-linked either physically or chemically. They consist mostly of water, which makes them similar to natural tissues. As a result of their remotely adaptable properties, they could form a foundation of a revolutionary drug delivery system for newly approved pharmaceuticals, such as recombinant proteins and peptides, monoclonal antibodies, and polynucleotides. Hydrogels possess the capacity to

encapsulate and protect drugs, leading to a diffusion-controlled sustained or spatial-temporal release of the active compound, which makes them a promising tool in the biopharmaceutical development [100]. A remarkably appealing feature of POx based hydrogels is the possibility of their injectability [101], accompanied with *in situ* gel formation due to LCST behavior, which can be triggered by physiological temperature. Such materials are referred to as thermoresponsive gels. In addition, this mechanism avoids the implantation of hydrogel in the body through invasive procedures. This adaptability and the absence of toxic cross-linkers and free radicals makes POx-based thermoresponsive hydrogels particularly suitable for drug delivery applications in nuclear medicine [100,102].

2.4.7 Poly(2-oxazoline) Hydrogel-based Drug Delivery System

In the last ten years, POx-based hydrogels have evolved from inert matrices to adjustable materials, which have proved to be therapeutically beneficial and therefore have been incorporated in clinical use as drug delivery systems. They are able to change behavior in response to one or combination of several stimuli, including pH and temperature such. Thermoresponsiveness can be significant for drug delivery systems, especially because it enables patient-specific kinetics [100,102]. Hydrogels provide spatial and temporal control over the release of various therapeutic agents, including radiolabeled compounds, which can serve for local radiotherapy [102-104]. Moreover, they are capable to co-deliver multiple drugs, with simultaneous imaging and therapeutical agents [100], which could extend their future applications in nuclear medicine e.g., as theranostics.

3 Experimental Part

3.1 Equipment and Materials

The ultrapure water was acquired from ELGA Purelab Ultra Scientific water purification system with 18.2 MΩ·cm resistivity. Polymer samples were lyophilized in either Heto Maxi Dry Lyo or Labconco FreeZone Plus 2.5 freeze dryer for sample drying in vacuum. The furan functionalized polymer was centrifuged in Sigma 2K15C centrifuge. The ^{1}H-NMR spectra were measured with 400 MHz NMR spectrometer, Bruker Avance NEO, for liquid state NMR measurement, provided with an autosampler and ^{1}H/(^{19}F,^{31}P-^{109}Ag) probe. The ^{15}N-NMR spectrum was measured with 500 MHz NMR spectrometer, Varian Unity Inova, for liquid state NMR measurement, provided with ^{1}H/^{13}C/^{15}N probe.

MS spectra were measured by MALDI-TOF-MS spectrometer in sinapic acid matrix at the Istitute of Organic Chemistry and Biochemistry CAS.

The radiolabeling experiments were performed with ^{68}Ga eluted with 0.1M HCl from ^{68}Ge/^{68}Ga IGG-100 generator by Eckert & Ziegler (Germany). The radiolabeled samples were incubated in Eppendorf ThermoMixer®/ ThermoStat C.

Measurements of buffer pH were performed with the Thermo Scientific™ Orion Star™ A111 Benchtop pH Meter with the glass Orion™ Green pH Combination Electrode. The pH value of radiolabeled solutions was tested with pH-indicator phenolphthalein paper with a color scale by MQuant®.

As a stationary phase, iTLC-SA glass microfiber chromatography (Agilent Technologies, Inc.) and Cytiva Whatman™ cellulose chromatography paper (with 0.18 mm film thickness) were used.

The TLC chromatograms of Experiments 1-19 were evaluated with Fujifilm FLA-5100 FLA Scanner for Digital Autoradiography (using 15 minutes development prior to the measurement). TLC chromatograms of Experiments 20-22 were scanned for 10 minutes with AR-2000 radio-TLC Imaging Scanner by Bioscan Inc.

Chelexed water was prepared with Chelex® 100 sodium form resins. All buffers were prepared with chelexed water.

Liquid chemicals such as acetic acid, citric acid, hydrochloric acid, ACN, chloroform, MeOH, EtOH, diethyl ether and THF as well as following solid chemicals ethyl-3-(furan-2yl)propionate, DTPA, EDTA, NaOH, NaCl, ammonium acetate (≥99,99%, trace metals basis), sodium acetate, sodium citrate, sodium phosphate dibasic heptahydrate, sodium phosphate monobasic monohydrate and sodium sulfate were purchased from Sigma-Aldrich®. DOTA-maleimide was obtained from CheMatech. All solutions and buffers were prepared with chemicals of highest purity.

Deuterated chloroform and deuterated methanol for ^{1}H-NMR analysis was obtained from Sigma-Aldrich®. Dialysis tubing cellulose membranes (3.5 kDa MWCO and 5 kDa MWCO) were purchased from Sigma-Aldrich®. SCX cartridge (Elut™-SCX with 100 mg and 1 ml capacity) was acquired from Agilent Technologies, Inc.

Ethyl-methyloxazoline$_{100}$-*b*-npropyloxazine$_{100}$-pipecolic acid polymer (P_0) was synthetized and characterized by Robert Luxenhofer et al. from University of Würtzburg, Faculty of Chemistry and Pharmacy.

DTPA-rituximab conjugate was prepared and characterized by Miroslav Vetrík et al. from Institute of Macromolecular Chemistry, Academy of Sciences of the Czech Republic.

Several buffers and mixtures were used for radiolabeling experiments and for TLC method development. For radiolabeling experiments, the following buffers were used: 0.5M Na-acetate (pH 4), 0.5M ammonium acetate (pH 4/pH 5), 1M/2.5M ammonium acetate (pH 5) and 0.5M phosphate buffer (pH 6/pH 7). For TLC method development, the following solutions were used as a mobile phase, 0.2M ammonium acetate buffer (pH 5), 0.2M Na-acetate buffer (pH 4), 1M Na-acetate + MeOH (1:1, by volume), 0.05M/0.2M Na-citrate buffer (pH 5), 0.1M Na-citrate buffer (pH 4), 5mM DTPA and MeOH/0.9M NaCl/EDTA [1 mg/µl] (9:1:0.5) mixture.

3.2 Methods and General Procedures

3.2.1 Partial Hydrolysis of Poly(2-oxazoline)

The hydrolysis reaction of methyl-methyloxazoline$_{100}$-*b*-npropyloxazine$_{100}$-pipecolic acid polymer (P_0) took place in acidic conditions. Firstly, 5 g of P_0 were dissolved in 50 ml of H_2O and the solution was heated to 70 °C using an oil bath. The temperature

was constantly monitored throughout the experiment and once it stabilized at 70 °C, 25 ml of concentrated HCl (37 %) were added, which initiated the hydrolysis. The desired hydrolysis degree was adjusted by controlling the reaction duration. The reaction was quenched after 13 minutes by transferring the mixture to an ice bath, followed by the addition of 25 ml of NaOH (20 wt%) to increase the pH above 10. After that, the excess water was removed from the reaction using a rotary evaporator (50 mbar, 50 °C, 60 rpm) for 3 hours.

To clean the hydrolysed polymer from formed impurities, a 48-hour long dialysis was performed using a 3.5kDa MWCO cellulose membrane, accompanied by gentle stirring. The polymer was then lyophilized with liquid nitrogen at low pressure (< 1 mbar). The degree of partial hydrolysis was determined using ^{1}H-NMR analysis, for which a small sample (~1 mg) was dissolved in 0.5 ml of deuterated chloroform.

3.2.2 Synthesis of 3-(2-Furyl)propionic Acid

To synthetize the 3-(2-furyl)propionic acid, 10 g (9.52 ml, 59.6 mmol) of ethyl-3-(furan-2yl)propionate was dissolved in 40 ml of THF. After that, 80 ml of 3M NaOH, dissolved in a mixture of H_2O:MeOH (1:1, by volume), were added. The solution was heated to 80 °C and stirred for 90 minutes. After cooling to room temperature, 80 ml of diethyl ether and 40 ml of 1M NaOH were added. The mixture was extracted, and the water phase was collected. Then, the water phase was extracted 3 times with 80 ml of diethyl ether and the combined organic phase was washed 3 times with 40 ml of 1M NaOH. The combined extracted water phase was then acidified to pH 1 with ~250 ml of 1M HCl and additionally extracted 4 times with 80 ml of diethyl ether. The organic phase was combined and washed with 10 ml of water. Then, the excess water was dried from the organic phase using Na_2SO_4, (2 spoons/100 ml) and filtered. The residual diethyl ether was evaporated from the mixture using a rotary evaporator (1 mbar, 110 °C, 60 rpm). A mixture of white/transparent crystals was obtained. A purifying distillation followed. The solid was molted and distilled at 110 °C at ~1 mbar. The structure of 3-(2-furyl)propionic acid was confirmed using ^{1}H-NMR analysis, for which a small sample (~1 mg) was dissolved in 0.5 ml of deuterated methanol.

3.2.3 Functionalization of Poly(2-oxazoline) with Furan

To functionalize a polymer with furan for a following DOTA-polymer modification, 1.9870 g of hydrolyzed P_0 was dissolved in 47 ml of ACN (0.002 M). The solution was cooled down in an ice bath, followed by the addition of a fourfold excess of both 0.077 g of DCC (0.4 mmol) and 0.052 g of 3-(2-furyl)propionic acid (0.4 mmol). The mixture was stirred in the dark overnight. A white solid substance precipitated and was subsequently removed by filtration. After that, ACN was removed with a rotary evaporator under reduced pressure (<250 mbar, 40 °C, 60 rpm) and the remaining viscous liquid was dissolved in ~6 ml of MeOH. The polymer solution was precipitated 2 times in 40 ml of an ice-cold diethyl ether and the precipitate was separated from the solvent with centrifugation (600 rpm for 15 minutes) and decantation. After that, the precipitate was dissolved in a small amount of water (~50 ml) and purified by dialysis using a 5 kDa MWCO cellulose membrane and gentle stirring for 72 hours. The acquired polymer was then lyophilized with liquid nitrogen at low pressure (< 1 mbar). The structure was confirmed with ^{1}H-NMR analysis, for which a small sample (~1 mg) was dissolved in 0.5 ml of deuterated chloroform.

3.2.4 DOTA Functionalization with the Diels-Alder Reaction

To perform the DA reaction, 96.5 mg of the furan-functionalized polymer (P_1) and 3.5 mg of DOTA-maleimide were dissolved in 2.23 ml of ACN and a few drops of chloroform, heated in an oil bath to 37 °C and stirred overnight in the dark. The acquired polymer solution was purified with dialysis in the dark for 24 hours using a 5 kDa MWCO cellulose membrane and gentle stirring, followed by lyophilization with liquid nitrogen at low pressure (< 1 mbar).

Approximately 1 mg of the acquired DOTA-modified polymer was dissolved in 0.5 ml of deuterated chloroform for ^{1}H-NMR and ^{15}N-NMR analysis. MALDI analysis was performed with saturated solution of synaptic acid.

3.2.5 Elution of ^{68}Ge/^{68}Ga Radionuclide Generator

The normal elution of the ^{68}Ge/^{68}Ga generator was performed using 0.1 M HCl. The eluate was collected in 1ml fractions. Usually, the 2nd or 3rd fraction was the most active and therefore used for the radiolabeling.

Concentrated elution of the generator was performed indirectly with the use of SCX cartridge, which was preconditioned with 1 ml of 5.5M HCl and washed with 10 ml of chelexed water prior to the elution step. After that, the generator was eluted with 10 ml of 0.1M HCl and ^{68}Ga was sorbed to the SCX cartridge. The cartridge was then eluted with a mixture of 12.5 µl of 5.5 M HCl in 0.5 ml of 5M NaCl solution. This eluate was used for ^{68}Ga radiolabeling.

3.2.6 Radiolabeling Procedures

3.2.6.1 Radiolabeling of DOTA-polymer with ^{68}Ga

Several radiolabeling experiments with DOTA-polymer were performed. The sample preparation for each experiment is listed in Tab. 2. The corresponding radiolabeling conditions are listed in Tab. 3. Parameters that were observed include type of ^{68}Ga elution, volume and activity of the ^{68}Ga eluate, concentration of the polymer in the sample, type and volume of the organic solvent, and type, concentration, pH and volume of the buffer. Also, the final pH of the mixture was studied including total time and temperature of the incubation.

Tab. 2: DOTA-polymer sample preparation for radiolabeling with ^{68}Ga.

Experiment	$m_{polymer}$ [mg]	Organic solvent	Buffer
1-12	0.25	70 µl EtOH	630 µl 0.5M Na-acetate (pH 4)
13-15	1.00	70 µl EtOH	630 µl 0.5M Na-acetate (pH 4)
16	1.00	70 µl EtOH	630 µl 0.5M ammonium acetate (pH 5)
17	1.00	70 µl EtOH	630 µl 1M ammonium acetate (pH 5)
18	1.00	70 µl EtOH	630 µl 2.5M ammonium acetate (pH 5)
19	2.00	70 µl EtOH	630 µl 0.5M ammonium acetate (pH 5)
20	1.00	350 µl EtOH	350 µl 0.5M ammonium acetate (pH 5)
21	1.00	350 µl EtOH	350 µl 0.5M ammonium acetate (pH 5)
22	1.00*	350 µl EtOH	350 µl 0.5M ammonium acetate (pH 5)

*unmodified polymer P_0

First, the respective amount of DOTA-polymer (m_{polymer}) was dissolved in the organic solvent. Then, the buffer was added to preserve the pH of the radiolabeling reaction, followed by the addition of certain volume of ^{68}Ga eluate (V_{eluate}). Prior to the incubation, the activity (A) of the mixture was measured on the NaI(Tl) scintillation well detector, followed by the pH test on a pH indicator paper. After that, the sample was transformed to the accordingly preheated Eppendorf ThermoMixer® and set to 500 rpm. The incubation was proceeded in the selected temperature (T) and for the

duration of chosen time (t). The incubation was either stopped and cooled down for 5 minutes or also quenched by the addition of 20 µl of 5 mM DTPA.

Tab. 3: Parameters of DOTA-polymer radiolabeling process with ^{68}Ga.

Experiment	Type of elution	V_{eluate} [µl]	A [MBq]	pH	T [°C]	t [min]	5 mM DTPA
1-12	normal	300	15	4	95	15	20 µl
13	normal	300	15	4	80		20 µl
14	normal	300	15	4	90		20 µl
15	normal	300	15	4	95		20 µl
16	normal	300	15	5	90		20 µl
17	normal	300	15	5	90		20 µl
18	normal	300	15	5	90		20 µl
19	concentrated	200	20	5	90		20 µl
20	normal	300	15	5	90		
21.1	normal	300	30	5	90		
21.2	normal	300	30	5	90		20 µl
22	normal	300	15	5	90		

3.2.6.2 Radiolabeling of DTPA-Rituximab Conjugate with ^{68}Ga

All radiolabeling experiments performed with DTPA-rituximab conjugate are listed in Tab. 4 and Tab. 5. Parameters that were observed include volume and activity of the ^{68}Ga eluate, concentration of the conjugate in the sample, as well as type, concentration, pH and volume of the buffer, and the final pH of the reaction mixture. Also, the incubation time and temperature was studied.

The acquired sample contained 10 mg/1 ml of dissolved DTPA-rituximab conjugate in 0.01M PBS buffer (pH 7.6). Firstly, 25 µl of DTPA-rituximab conjugate ($V_{\text{conjugate}}$) were added to 675 µl of selected buffer solution. Then, 300 µl of ^{68}Ga eluate were added and the activity (A) of the mixture was measured on the NaI(Tl) scintillation well detector, followed by the pH test on a pH indicator paper. The sample was transformed to the Eppendorf ThermoMixer® preheated to T=37 °C and set to 500 rpm. Several incubation durations were tested in dependency on pH.

Tab. 4: DTPA-rituximab conjugate sample preparation for radiolabeling with ^{68}Ga.

Experiment	$V_{\text{conjugate}}$ [µl]	Buffer
I	0.25	675 µl 0.5M ammonium acetate (pH 4)
II		675 µl 0.5M ammonium acetate (pH 5)
III		675 µl 0.5M phosphate (pH 6)
IV		675 µl 0.5M phosphate (pH 7)

Tab. 5: Parameters of DTPA-rituximab conjugate radiolabeling process with ^{68}Ga.

Experiment	Type of elution	V_{eluate} [µl]	A [MBq]	pH	T [°C]
I/V/IX	normal	300	20	4	37
II/VI/X				5	
III/VII/XI				6	
IV/VIII/XI				7	

In Experiments V-VIII, where formation of ^{68}Ga-colloid was studied, the volume of the selected buffer was increased to 700 µl in each sample and other parameters remained the same. In experiments IX-XII, where the behavior of free DTPA was studied, 25 µl of 5mM DTPA solution was used instead of the conjugate and other parameters remained the same.

3.2.7 TLC Methods

For the quality control of the radiolabeled DOTA-polymer and DTPA-rituximab conjugate, respectively, a TLC method was utilized. In this thesis, various TLC methods were tried in Experiments 1-11 before developing a suitable candidate for a clear separation of the free ^{68}Ga and the radiolabeled compound. Starting with Experiment 12 all following TLC methods were performed with Whatman® cellulose chromatography paper as the stationary phase and 0.2M sodium citrate buffer (pH 5) as the mobile phase. All studied methods and corresponding experiments are listed in Tab. 6.

Tab. 6: Tested combinations of a stationary phase and a mobile phase of TLC analysis.

Experiment	Stationary phase	Mobile phase
1	iTLC-SA	0.2M ammonium acetate buffer (pH 5)
2	iTLC-SA	0.2M Na-acetate buffer (pH 4)
3	iTLC-SA	1M Na-acetate + MeOH (1:1, by volume)
4	iTLC-SA	0.05M Na-citrate buffer (pH 5)
5	iTLC-SA	0.1 Na-citrate buffer (pH 4)
6	iTLC-SA	0.2M Na-citrate buffer (pH 5)
8	iTLC-SA	5mM DTPA
9	iTLC-SA	MeOH/0.9M NaCl/EDTA [1 mg/µl] (9:1:0.5)
10	Whatman®	1M Na-acetate + MeOH (1:1, by volume)
11	Whatman®	5mM DTPA
12-22	Whatman®	0.2M Na-citrate buffer (pH 5)

For each TLC analysis, a drop (~2 µl) of radiolabeled mixture was transferred on the base of the TLC plate, which was 2 cm wide and 10 cm long. The stationary phase was then placed inside an incubation cell, with approximately 1 ml of mobile phase, until

the mobile phase reached the front of the TLC plate. The developed plate was then measured using a respective TLC scanner. Peak areas were integrated to estimate the radiolabeling yield. For statistical purposes, relative standard deviation approach developed in the literature for TLC analysis [105] was utilized, where seven measurable sources of uncertainty were described (Tab. 7) and calculated according to the propagation of uncertainty

$$u^2 = \sum_i \left(\frac{\partial y}{\partial x_i}\right)^2 \cdot u_{x_i}^2, \tag{3}$$

where u represents the standard deviation of the combined uncertainties, $\frac{\partial y}{\partial x_i}$ is a partial derivative of $y = f(x_i)$ with respect to the i^{th} variable, and u_{x_i} is the uncertainty of the i^{th} variable. The resulting total standard deviation of the radiolabeling yield was estimated as u = 4.5 %.

Tab. 7: Measurable sources of uncertainty resulting from sample preparation for TLC analysis with corresponding relative standard deviations $\boldsymbol{u_{x_i}}$ [105].

$\boldsymbol{i^{\text{th}}}$ **variable of sample preparation**	$\boldsymbol{u_{x_i}}$ **[%]**
weighing	0.5
dilution	1.0
TLC plate selection	0.2
vertical chromatography development	1.0
drying in cold air	1.5
scanner	0.1
integration	0.2

4 Results and Discussion

4.1 Synthesis of DOTA-polymer

4.1.1 Partial Hydrolysis of Poly(2-oxazoline)

The partial hydrolysis of 5 g of P_0, which is equal to a total amide concentration of 0.48 M, resulted in the formation of 4.7 g of hydrolysed polymer (yield = 94 %). The degree of hydrolysis was estimated using the ^{1}H-NMR analysis, which is shown in Fig. 4. It was calculated as 2.1 %, which is equal to the ratio of the integral of peaks 4 and 1. Peak 4 corresponds to the newly formed amide and peak 1 to the ethyl side chain.

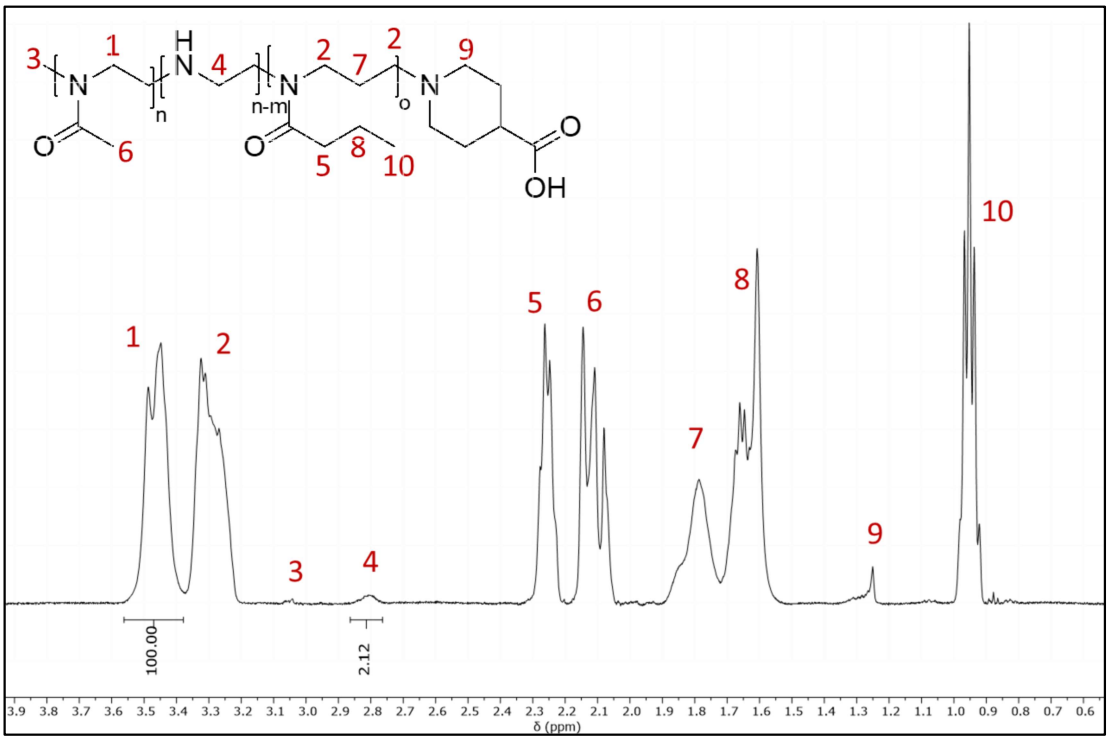

Fig. 4: ^{1}H-NMR analysis and structure of partially hydrolysed POx based polymer, δ (ppm): 3.6-3.4 (100H, **1**), 3.6-3.2 (**2**), 3.05 (**3**), 2.85-2.75 (2H, **4**), 2.35-2.2 (**5**), 2.17-2.05 (**6**), 1.9-1.73 (**7**), 1.7-1.55 (**8**), 1.3-1.24 (**9**), 1-0.9 (**10**).

4.1.2 Synthesis of 3-(2-Furyl)propionic Acid

For the synthesis, 10 g (9,52 ml, 59,6 mmol) of ethyl-3-(furan-2yl)propionate were used, which resulted in the preparation of 7.92 g of 3-(2-furyl)propionic acid. The yield was 79 %. The structure was confirmed using ^{1}H-NMR analysis. The spectrum is shown in Fig. 5.

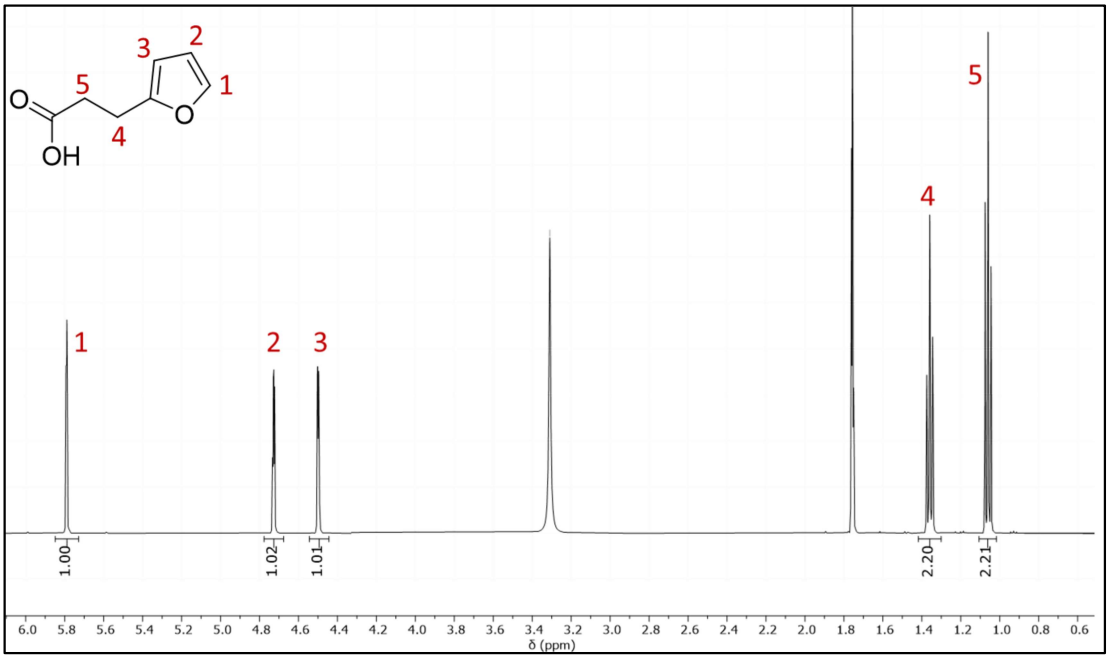

Fig. 5: ^{1}H-NMR spectrum and structure of 3-(2-furyl)propionic acid, δ (ppm): 5.8 (1H, **1**), 4.75 (1H, **2**), 4.5 (1H, **3**), 1.35 (2H, **4**), 1.05 (2H, **5**).

4.1.3 Functionalization of Poly(2-oxazoline) with Furan

The synthesis started with 1.9870 g of hydrolyzed P_0 (0.1 mmol of the respective amine concentration) and resulted in preparation of 108.7 mg of furan-functionalized methyl-methyloxazoline$_{99}$-*stat*-furanoxazoline$_1$-*b*-npropyloxazine$_{100}$-pipecolic acid polymer = P_1. The yield was 5.5 %. The ^{1}H-NMR analysis is shown in Fig. 6. To confirm the furan-functionalization, signals from furan (peaks 1, 2) were used.

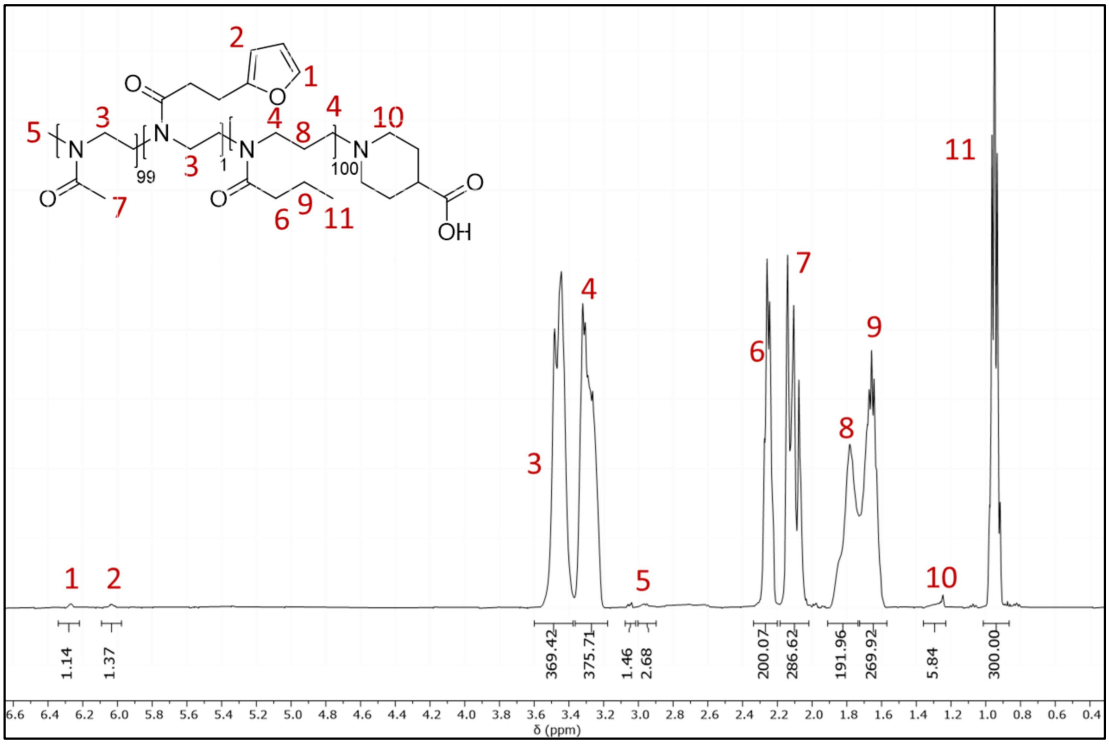

Fig. 6: ^{1}H-NMR analysis and structure of furan-functionalized POx based polymer, δ (ppm): 6.35-6.2 (1H, **1**), 6.1-6 (1H, **2**), 3.6-3.4 (369H, **3**), 3.4-3.2 (376H, **4**), 3.1-2.95 (3H, **5**), 2.3-2.2 (200H, **6**), 2.17-2 (287H, **7**), 1.9-1.7 (192H, **8**), 1.7-1.55 (270H, **9**), 1.35-1.25 (6H, **10**), 1-0.9 (300H, **11**).

4.1.4 DOTA Functionalization with the Diels-Alder Reaction

The DA reaction with 96.5 mg of the furan-functionalized polymer and 3.5 mg of DOTA-maleimide resulted in the preparation of 65.3 mg of DOTA-polymer; the yield was 65.3 %. The structure is shown in Fig. 7. The calculated molecular weight is approximately 21 kDa. The performed ^{1}H-NMR and ^{15}N-NMR analysis could not confirm the polymer structure because the DOTA group signal was too low to be recognized in the spectra. MALDI analysis also did not positively confirm the occurrence of DOTA, because the assigned peak was too wide as is shown in Fig. 8. The conclusion was that due to the click chemistry of the DA reaction, the DOTA modification should have been successful, however the upcoming radiolabeling reactions with ^{68}Ga would confidently confirm the hypothesis.

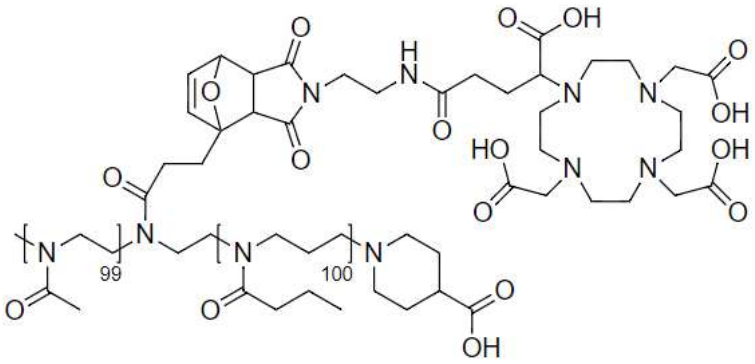

Fig. 7: The supposed structure of a DOTA-modified POx based polymer prepared by the DA reaction.

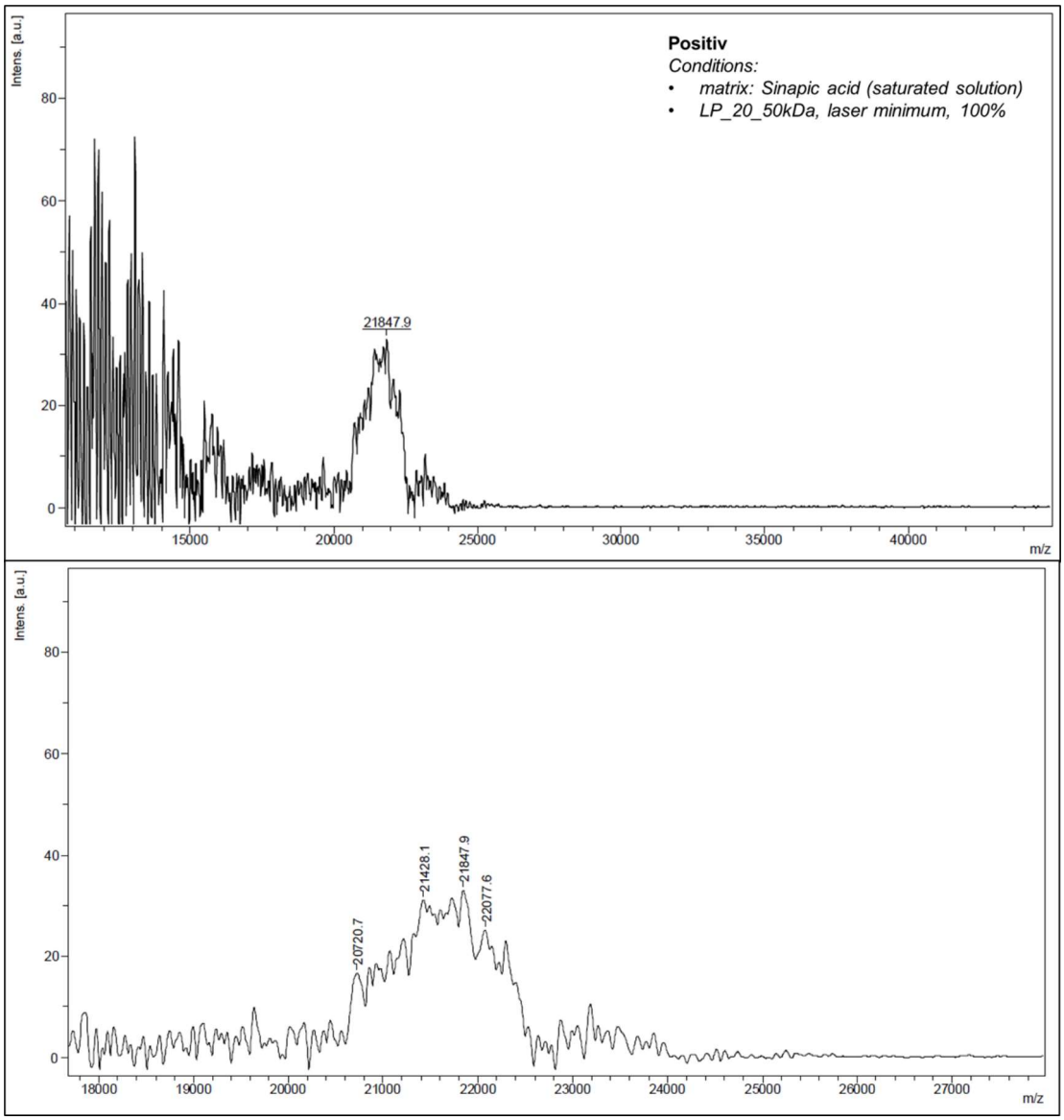

Fig. 8: MALDI analysis of DOTA-modified polymer (above) with DOTA-assigned peak close up (below).

4.2 DOTA-polymer Radiolabeling Process and TLC Method Development

In the first twelve experiments (experiments 1-12), the attention was focused on TLC method development to achieve a clear and rapid visualization of the radiolabeling efficiency and therefore confirm the speculations, whether the DOTA-polymer modification had been successful. The speculations were appropriate because so far, all analyses of the DOTA-polymer (^{1}H-NMR, ^{15}N-NMR, MALDI) only suggested a promising occurrence of the DOTA group at the polymer chain but were inconclusive.

The radiolabeling of DOTA modified POx-based polymer with ^{68}Ga has not been described in the literature yet. For that reason, the development of radiolabeling process was based on the ^{68}Ga-DOTATOC. Food and Drug Administration (FDA) approved and routinely utilized method and on ^{68}Ga-DOTA radiolabeling chemistry, where elevated temperature of 95 °C and acidic pH is required to achieve an efficient chelation of the radiometal. This approach was later amended in the favor of the highest radiolabeling yields, however, for experiments 1-12, 95 °C was used as the incubation temperature. The choice of a reaction buffer was based on ^{68}Ga chemistry. The intention was to provide suitable environment for the chelation to outcompete the formation of $^{68}Ga(OH)_3$, which begins to precipitate at pH ≥ 3. Experiments 1-12 were performed with 630 µl of 0.5M sodium acetate buffer (pH 4.0). Ethanol (10 µl) was included in the mixture as an organic solvent of the DOTA-polymer to prevent hydrogelation of the polymer *in vitro* during incubation. The volume of the ^{68}Ga eluate (300 µl) was adjusted to contain enough activity for the reaction mixture (A = 15 MBq) and according to the buffer capacity, which otherwise could have been broken with an addition of a larger volume of a strong acid (>300 µl of 0.1M HCl).

In the search of an ideal TLC method that shows a well-defined separation of the free ^{68}Ga and the radiolabeled DOTA-polymer, several unsuccessful combinations of stationary phase and mobile phase were tested and ruled out in experiments 1-11. The molar mass of the DOTA-polymer (~21 kDa) suggested that the polymer is more likely to stay on the base of the TLC chromatogram. For that reason, the intention was to move the ionic $^{68}Ga^{3+}$ with the mobile phase to the front. The addition of 20 µl of 5 mM DTPA was included at the end of the incubation to quench the radiolabeling

reaction and to carry the ionic $^{68}Ga^{3+}$ to the front, which provided a better resolution of the two acquired peaks in the chromatogram (Fig. 12).

Comparison of the obtained TLC chromatograms from experiments 1-12 showed that the finest separation of the radiolabeled DOTA-polymer and free ^{68}Ga was achieved using Whatman® cellulose chromatography paper as stationary phase and 0.2M sodium citrate buffer (pH 5.4) as mobile phase, which is analogical to one of the two methods used for quality control of ^{68}Ga-DOTATOC (a glass-fiber ITLC paper as stationary phase and 0.1M sodium citrate, pH 5 as mobile phase) [56]. This method ensures that DOTA-polymer stays on the base and free $^{68}Ga^{3+}$ moves with the front. Unfortunately, no TLC method that would allow the ^{68}Ga-colloid move with the front has been described in the literature yet and therefore, the formed $^{68}Ga(OH)_3$ potentially improved the radiolabeling yield on the base. Most tested methods with iTLC-SA as a stationary phase showed only one peak at the base or several peaks throughout the chromatogram, which is illustrated in Fig. 9. The separation was therefore unsuccessful, and the results were inconclusive.

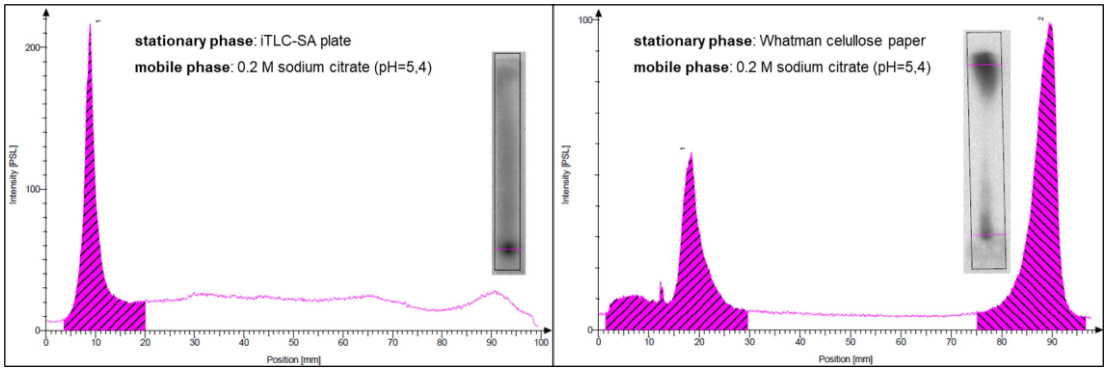

Fig. 9: A TLC method development (left: iTLC-SA as a stationary phase combined with 0.2M Na-citrate as a mobile phase with apparent smudges across the chromatogram; right: Whatman® cellulose chromatography paper as a stationary phase combined with 0.2M Na-citrate as a mobile phase with no apparent smudges across the chromatogram).

Once the reliable and efficient TLC method was developed, it was time to optimize the sample preparation and the radiolabeling process. First, the incubation temperature was investigated. Different elevated incubation temperatures (80 °C, 90 °C and 95 °C) were studied in experiments 13-15 to examine the hypothesis that incubation at 95 °C is the most appropriate for efficient ^{68}Ga-DOTA chelation. The concentration of the polymer in each sample was increased from 0.25 mg to 1 mg (Tab. 3). The conclusion

was that no significant difference in the radiolabeling efficiency was found among the tested temperatures. The observation was based on the calculated radiolabeling yield (Y) and on the separation of DOTA-polymer and free ^{68}Ga on all acquired chromatograms, which showed resemblance (Fig. 10). The highest radiolabeling yield $Y = 42.5 \pm 1.9$ % (Tab. 8) was obtained from experiment 14, which was incubated at 90 °C. For that reason, incubation at 90 °C was utilized for all upcoming experiments that were performed at elevated temperature.

Tab. 8: Radiolabeling yields (Y) of experiments with polymer.

Experiment	Buffer	Y [%]
13	630 µl 0.5M Na-acetate (pH=4)	33.6±1.5
14	630 µl 0.5M Na-acetate (pH=4)	42.5±1.9
15	630 µl 0.5M Na-acetate (pH=4)	32.0±1.4
16	630 µl 0.5M ammonium acetate (pH=5)	25.5±1.1
17	630 µl 1M ammonium acetate (pH=5)	19.9±0.9
18	630 µl 2.5M ammonium acetate (pH=5)	5.7±0.3
19	630 µl 0.5M ammonium acetate (pH=5)	30.7±1.4
20	350 µl 0.5M ammonium acetate (pH=5)	52.7±2.4
21.1	350 µl 0.5M ammonium acetate (pH=5)	60.5±2.7
21.2	350 µl 0.5M ammonium acetate (pH=5)	64.8±2.9
22*	630 µl 0.5M ammonium acetate (pH=5)	8.6±0.4

*unmodified P_0

As the incubation temperature was optimized, the next step was to improve the radiolabeling yield to exceed 45 % (Tab. 8). The idea was to change the buffer from 0.5M sodium acetate (pH 4) to ammonium acetate (pH 5) to remove additional metal ions (Na^+) from the reaction mixture. In addition, the pH of the buffer was increased. While the precipitation of ^{68}Ga-colloid increases rapidly with pH closer to neutral, mild pH is desirable for pharmaceuticals with potential intravenous applications, because they are less likely to provoke an undesirable reaction *in vivo*. As a result, pH 5 was more appropriate to study. With the increased temperature, the DOTA chelation should outcompete the $^{68}Ga(OH)_3$ formation. In experiments 16-18, 0.5M, 1M and 2.5M ammonium acetate buffer were examined. The highest radiolabeling yield $Y = 25.5 \pm 1.1$ % (Tab. 8) showed sample in experiment 16 with 0.5M ammonium acetate in the mixture (Fig. 11). This buffer was used in the following experiments.

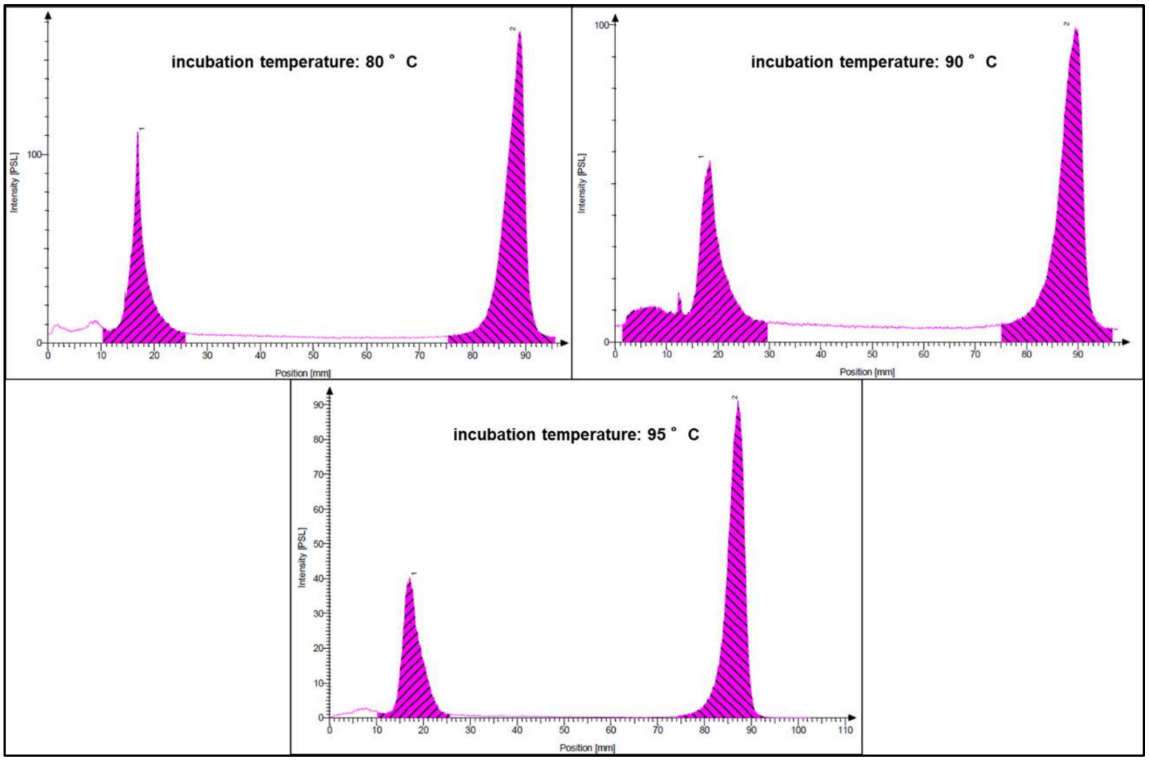

Fig. 10: TLC chromatograms of experiments 13-15 incubated at 80 °C (top left), 90 °C (top right) and 95 °C (bottom).

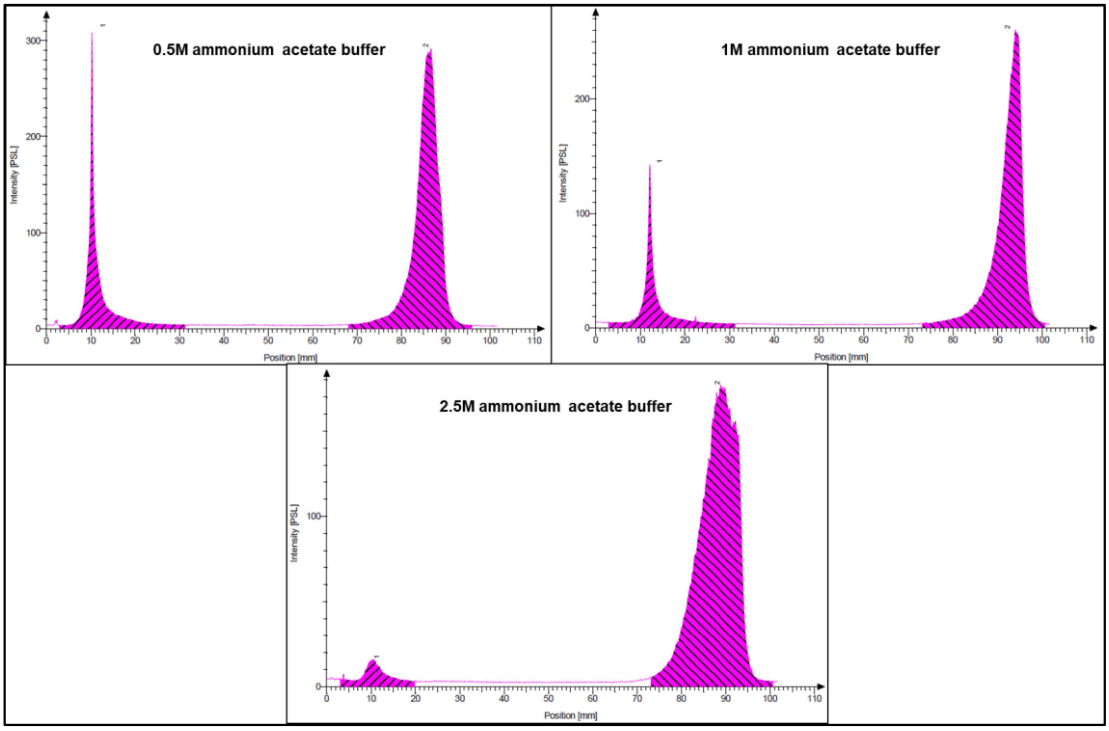

Fig. 11: TLC chromatograms of experiments 16-18 with ammonium acetate buffer of different concentration: 0.5M (top left), 1M (top right) and 2.5M (bottom).

To improve the radiolabeling yield, concentrating the ^{68}Ga elution for experiment 19 was tried to obtain higher activity in a lower elution volume. Also, the concentration

of the polymer in a sample was increased to 2 mg. Interestingly, the obtained radiolabeling yield Y = 30.7 ± 1.4 % (Tab. 8) did not significantly improve. For the experiments 20-21 a different approach was tested. The volume of EtOH as organic solvent was increased to 350 µl and the volume of 0.5M ammonium acetate buffer was decreased to 350 µl (1:1, by volume). In experiment 20, the activity of the eluate was 15 MBq and in experiment 21 it was doubled to 30 MBq. The experiments were successful and resulted in notably higher radiolabeling yields $Y_{\mathrm{Ex.20}}$ = 52.7 ± 2.4 % for experiment 20 and $Y_{\mathrm{Ex.21a}}$ = 64.8 ± 2.9 % for experiment 21.1, which corresponds to the increased concentration of ^{68}Ga available for the radiolabeling reaction. The 20 µl of 5mM DTPA addition prior to the TLC analysis was excluded from these experiments. As is apparent from the Fig. 12, the 5mM DTPA addition only improves the resolution of the TLC separation and provides equivalent radiolabeling result (Tab. 8, experiment 21.2). In the upcoming experiments, even higher activity obtained with e.g., concentrated elution, should be tested to confirm the growing radiolabeling yield trend.

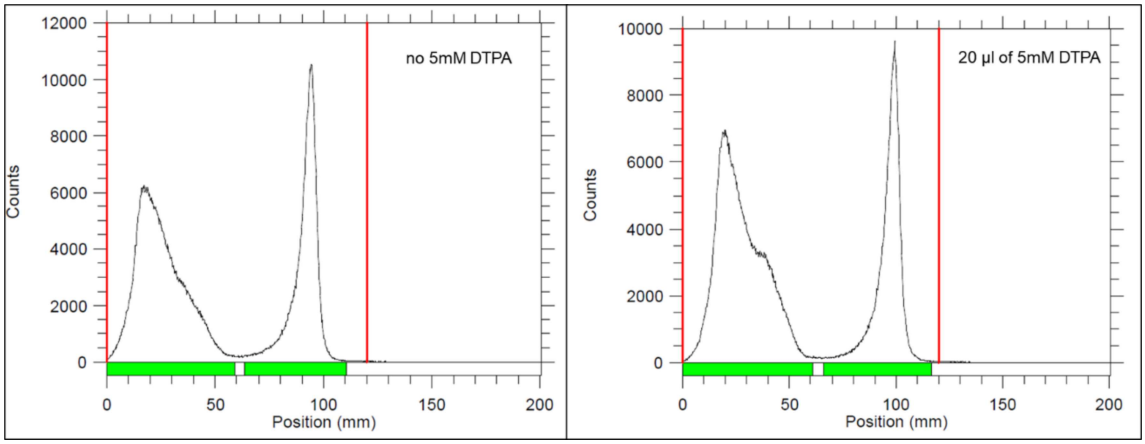

Fig. 12: TLC chromatograms of experiments 20 and 21.2 with optimized radiolabeling conditions (left: without DTPA addition right: with DTPA addition prior to the TLC analysis).

With adjusted sample preparation and radiolabeling conditions, experiment 22 was performed to compare radiolabeling efficiency of DOTA-polymer and unmodified polymer P_0 to resolve the question, whether the DA reaction was successful. The results clearly demonstrate that DOTA-polymer shows a significantly higher radiolabeling yield (experiment 20) than unmodified P_0 (experiment 22), where the yield was only $Y_{\mathrm{Ex.22}}$ = 8.6 ± 0.4 % (Tab. 8). This experiment confirms the DOTA chelator presence on the polymer chain.

4.3 DTPA-rituximab Radiolabeling Process

The next part of this thesis was focused on development of the ideal ^{68}Ga radiolabeling conditions for DTPA-rituximab conjugate. This compound should be attached to POx based polymer in the future work and be tested as a potential diagnostic radiopharmaceutical for patients with CD20 positive B cell NHL.

Several radiolabeling experiments with ^{68}Ga were performed, investigating time and pH dependence of the reaction. For quality control and radiolabeling yield estimation a TLC method developed in the previous chapter of this thesis was utilized. The radiolabeled DTPA-rituximab conjugate, with molecular weight approximately 150 kDa, stayed on the base of the TLC plate and free ionic $^{68}Ga^{3+}$ moved with the front.

Tab. 9: The ^{68}Ga radiolabeling yield [%] of DTPA-rituximab conjugate in dependency on time and the pH of the reaction mixture.

Experiment	pH	6 min	12 min	18 min	24 min	30 min
I	4	96.9±3.1	96.4±3.6	97.1±2.9	96.2±3.8	97.3±2.7
II	5	56.7±2.6	52.4±2.4	53.6±2.4	52.2±2.3	56.7±2.6
III	6	2.7±0.1	4.7±0.2	3.8±0.2	4.5±0.2	8.6±0.4
IV	7	1.4±0.1	1.8±0.1	5.4±0.2	2.6±0.1	4.2±0.2

The results of radiolabeling experiments with DTPA-rituximab conjugate (Tab. 9) suggest that the ideal pH for ^{68}Ga radiolabeling is 4, where the radiolabeling efficiency was potentially 100 % within 6 minutes. While pH 5 also gives promising results, the radiolabeling yields were nearly half the previous values. Despite that, pH 5 provides more suitable environment for mAb radiolabeling, because the antibody is a fragile biomaterial that is very sensitive to extreme conditions such as elevated temperature or strongly acidic pH. For this reason, even milder pH > 5 would be more appropriate for the radiolabeling reaction, but unfortunately, the radiolabeling yield was very low at pH 6 and 7. The results of experiments III and IV were inconsistent, most likely because of the poor formation of ^{68}Ga-DTPA-rituximab complex, which was distributed in the mixture in very low concentrations alongside ^{68}Ga-colloid. Therefore, in experiments V-VIII, the formation of ^{68}Ga-colloid was studied to discover a possible increase in the radiolabeling yield on the base of the TCL chromatograms. To have a better understanding of the radiolabeling process, reaction of ^{68}Ga eluate in each buffer was examined. The results (Tab. 10) are positively

different from expectations. A trend can be observed in results of experiment V, but considerable inconsistency is showed in experiments VI-VIII. The explanation for oscillating numbers in experiments VI-VIII would be the presence of dynamic chemical equilibrium of the reaction in dependence on pH and time. Experiment V shows the time dependent increasing precipitation of ^{68}Ga-colloid in the reaction mixture which was expected.

To summarize, after the comparison of the results from experiments I-IV and experiments V-VIII, the formation of ^{68}Ga-colloid does not gradually and falsely improve the radiolabeling yield of ^{68}Ga-DTPA-rituximab complex. The DTPA chelation most likely outcompetes the ^{68}Ga-colloid formation when the DTPA-rituximab is present in the reaction mixture.

Tab. 10: Time and pH dependency of ^{68}Ga-colloid formation [%] on the base of TLC chromatogram.

Experiment	pH	0 min	6 min	15 min
V	4	14.3±0.6	19.3±0.9	74.5±3.4
VI	5	10.7±0.5	1.1±0.1	18.2±0.8
VII	6	1.7±0.1	4.2±0.2	0.0±0.0
VIII	7	39.4±1.8	5.2±0.1	0.6±0.0

To demonstrate the pH and time dependency of ^{68}Ga-DTPA-rituximab complex chelation efficiency in experiments I-IV and of ^{68}Ga-colloid formation in experiments V-VIII, corresponding diagrams were plotted in Fig. 13 and Fig. 14.

Experiments IX-XII were performed under the same conditions as experiments I-IV but with the addition of 25 µl of 5mM DTPA instead of 25 µl of the conjugate to investigate the behavior of free DTPA in the reaction mixture, to prove the strength of DTPA-rituximab bond in different pH. The yield of experiments IX-XII was $Y = 100\ \%$ in the front of the TLC chromatograms in all investigated times (t = 0, 6, 12, 18, 30 min). The results show that the efficiency of ^{68}Ga-DTPA chelation is triggered instantly and that DTPA forms a strong, stable and time independent complex with ^{68}Ga at pH 4, 5, 6 and 7. The experiments also prove that the DTPA-rituximab bond does not break in the experiments, otherwise no radiolabeling yield would be obtained on the base of the chromatograms during experiments I-IV.

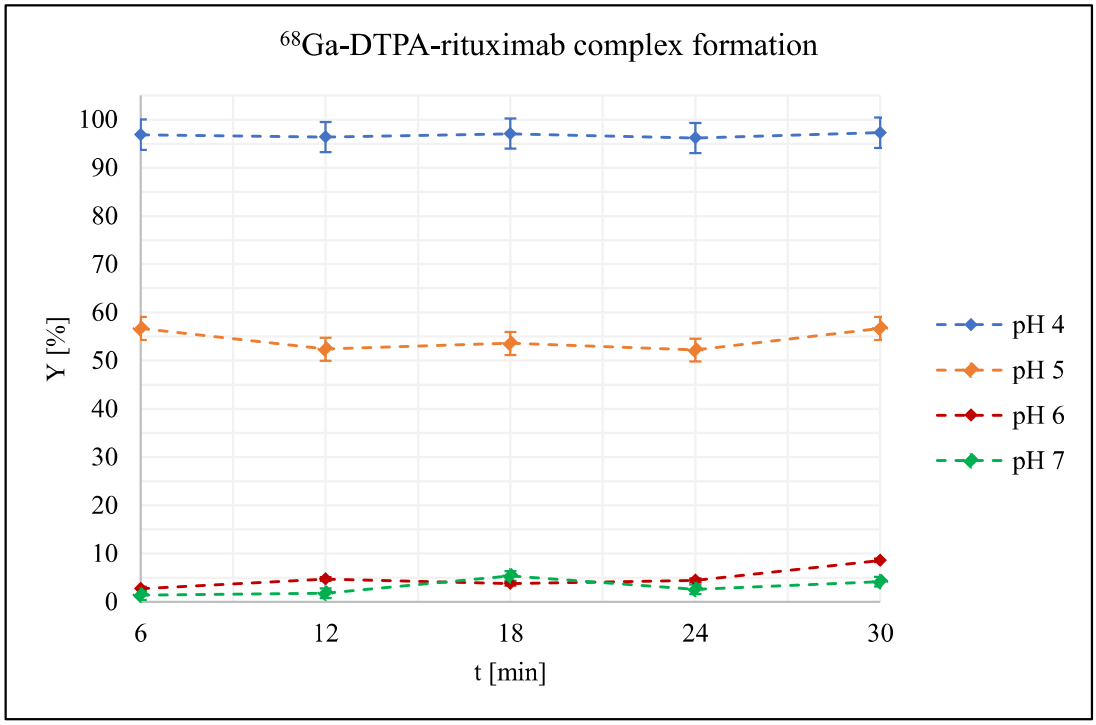

Fig. 13: Time and pH dependence of ^{68}Ga-DTPA-rituximab complex formation.

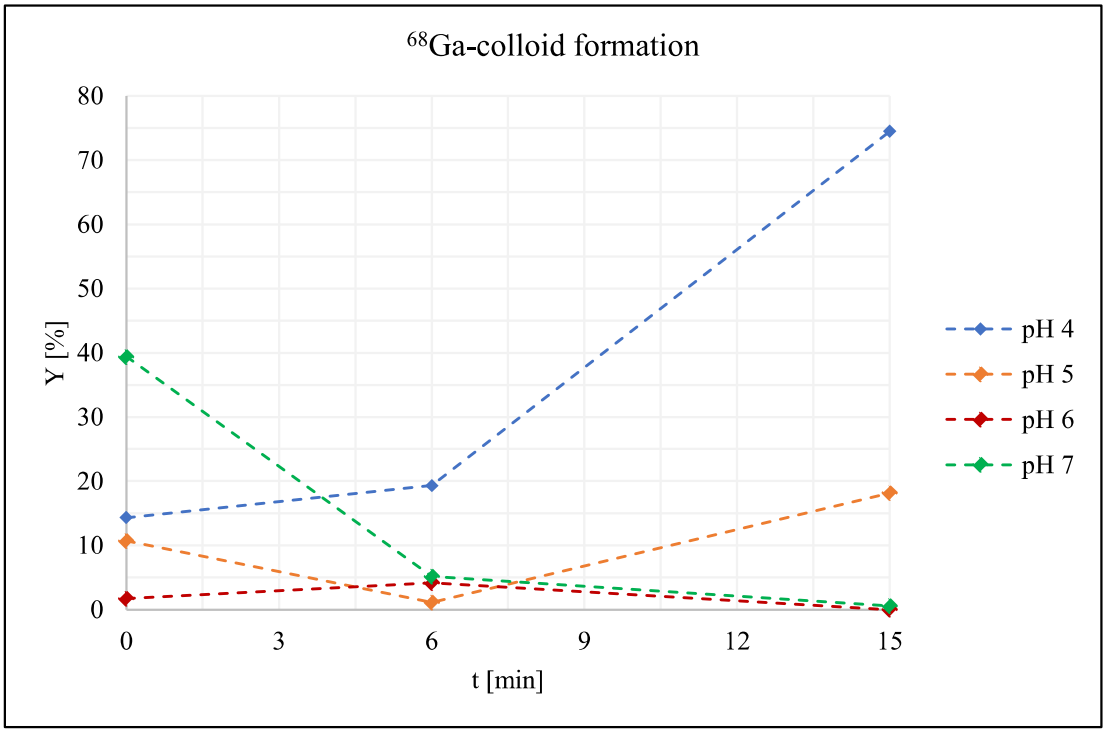

Fig. 14: Time and pH dependence of ^{68}Ga-colloid formation.

5 Conclusion

This thesis reviewed the obstacles of ^{68}Ga-radiolabeled POx-based polymer preparation. During the process:

1. a TLC method for macromolecules radiolabeled with ^{68}Ga was developed,
2. ideal ^{68}Ga radiolabeling conditions for POx-based DOTA-polymer were found,
3. the formation of ^{68}Ga-colloid in solutions with different pH was determined,
4. various ^{68}Ga radiolabeling conditions for DTPA-rituximab conjugate were studied,
5. and DTPA-rituximab stability in solutions with different pH was evaluated.

For the TLC analysis Whatman® cellulose chromatography paper served as the stationary phase and 0.2M Na-citrate was the mobile phase. The radiolabeled compound stayed on the base of the chromatogram and the ionic ^{68}Ga moved with the front.

The ideal ^{68}Ga radiolabeling conditions for examined DOTA-polymer were the following: to dissolve 1 mg of the DOTA-polymer, 350 µl of EtOH as organic solvent and 350 µl of 0.5M ammonium acetate buffer (pH 5) were used. The activity of the ^{68}Ga eluate was 30 MBq in 300 µl volume. The incubation was proceeded at 90 °C for 15 minutes. The radiolabeling yield was $Y = 64.8 \pm 2.9$ %. In the upcoming experiments, even higher activity obtained with e.g., concentrated elution, should be tested to investigate the hypothesis that radiolabeling yield was growing with the increasing eluate activity. Once the yield of ^{68}Ga radiolabeling experiments reaches maximum i.e., the DOTA vacancies available on the polymer chain are saturated and the yield is sufficiently stabilized, purification of the ^{68}Ga-DOTA-polymer would be appropriate. Consequently, the *in vivo* experiments should follow to observe the biokinetics of the developed radiopharmaceutical. Those experiments were not performed and summarized in this thesis because of the lengthy research that was associated with the optimization of the DOTA-polymer radiolabeling experiments. Nevertheless, they will be an inevitable part of the future work.

In case that the maximal yield of the DOTA-polymer radiolabeling experiments has already been obtained and will not increase further, the benefits of potential NOTA-polymer modifications instead of DOTA should not be overlooked. Many

obstacles would be solved, because NOTA provides more stable and inert complex with ^{68}Ga and the radiolabeling reaction can be proceed at room temperature. Therefore, the potential occurrence of the reversed DA reaction at elevated temperature would not be a thread.

To summarize the DTPA-rituximab radiolabeling experiments, the observation was that the ^{68}Ga-DTPA-rituximab complex could be formed rapidly within 6 minutes. The ideal pH for the radiolabeling reaction was pH 4 which provided superior radiolabeling results at all investigated times, however pH 5 should be studied further. The DTPA-rituximab bond did not break at pH 4, 5, 6 and 7. In future experiments, the survival rate of rituximab in acidic conditions should be studied to confirm that pH 4 or 5 is suitable for further ^{68}Ga-DTPA-rituximab radiopharmaceutical development.

Experiments performed with DTPA-rituximab showed the benefits of ^{68}Ga-DTPA chelation over ^{68}Ga-DOTA chelation. The reaction was rapid, effective and could have been proceeded under mild conditions (37 °C). More ^{68}Ga radiolabeling experiments with DTPA conjugated to biological materials should be investigated in the future, for potential applications in PET radiodiagnostics. In addition, conjugation of DTPA-rituximab to POx based polymer could provide protection for the radiolabeled mAb *in vivo*, because the hydrogelation of the POx could shield rituximab from the surrounding environment.

6 Bibliography

[1] Nuclear medicine and PET/CT: technology and techniques. Eighth edition. Editor Kristen M. WATERSTRAM-RICH, editor David GILMORE. St. Louis: Elsevier, 2017. [cit. 2022-03-17]. ISBN 978-0-323-35622-0.

[2] OECD *Health Statistics 2021*, "Positron Emission Tomography (PET) exams", in Health Care Utilisation [cit. 2022-03-17]. Available from: https://stats.oecd.org/index.aspx?queryid=30160

[3] CHERRY, Simon R. and Magnus DAHLBOM. PET: Physics, Instrumentation, and Scanners. PHELPS, Michael E., ed. PET [online]. New York, NY: Springer New York, 2006, s. 1-117 [cit. 2022-03-17]. ISBN 978-0-387-32302-2. doi:10.1007/0-387-34946-4_1

[4] KAPOOR, Vibhu, Barry M. MCCOOK and Frank S. TOROK. An Introduction to PET-CT Imaging. RadioGraphics [online]. 2004, 24(2), 523-543 [cit. 2022-03-17]. ISSN 0271-5333. doi:10.1148/rg.242025724

[5] FANI, Melpomeni, João P. ANDRÉ and Helmut R. MAECKE. ^{68}Ga-PET: a powerful generator-based alternative to cyclotron-based PET radiopharmaceuticals. Contrast Media & Molecular Imaging [online]. 2008, 3(2), 53-63 [cit. 2022-03-18]. ISSN 15554309. doi:10.1002/cmmi.232

[6] LORSON, Thomas, Michael M. LÜBTOW, Erik WEGENER, et al. Poly(2-oxazoline)s based biomaterials: A comprehensive and critical update. Biomaterials [online]. 2018, 178, 204-280 [cit. 2022-03-18]. ISSN 01429612. doi:10.1016/j.biomaterials.2018.05.022

[7] GAERTNER, Florian C., Robert LUXENHOFER, Birgit BLECHERT, Rainer JORDAN and Markus ESSLER. Synthesis, biodistribution and excretion of radiolabeled poly(2-alkyl-2-oxazoline)s. Journal of Controlled Release [online]. 2007, 119(3), 291-300 [cit. 2022-03-18]. ISSN 01683659. doi:10.1016/j.jconrel.2007.02.015

[8] GODDARD, Peter, Lusie E. HUTCHINSON, Janet BROWN and Laurence J. BROOKMAN. Soluble polymeric carriers for drug delivery. Part 2. Preparation and in vivo behaviour of N-acylethylenimine copolymers. Journal of Controlled Release [online]. 1989, 10(1), 5-16 [cit. 2022-03-18]. ISSN 01683659. doi:10.1016/0168-3659(89)90013-8

[9] BERRY, David J., Yongmin MA, James R. BALLINGER, et al. Efficient bifunctional gallium-68 chelators for positron emission tomography: tris(hydroxypyridinone) ligands. Chemical Communications [online]. 2011, 47(25) [cit. 2022-03-18]. ISSN 1359-7345. doi:10.1039/c1cc12123e

[10] CHAKRAVARTY, Rubel, Sudipta CHAKRABORTY, Ashutosh DASH and M.R.A. PILLAI. Detailed evaluation on the effect of metal ion impurities on complexation of generator eluted ^{68}Ga with different bifunctional chelators. Nuclear Medicine and Biology [online]. 2013, 40(2), 197-205 [cit. 2022-03-19]. ISSN 09698051. doi:10.1016/j.nucmedbio.2012.11.001

[11] ADAM J., KADEŘÁVEK J., KUŽEL F., VAŠINA J. and ŘEHÁK Z. Current Trends in Using PET Radiopharmaceuticals for Dia gnostics in Oncology. Regionální centrum aplikované molekulární onkologie, Masarykův onkologický ústav, Brno, 2014. Available at: https://www.linkos.cz/files/klinicka-onkologie/186/4505.pdf [cit. 2022-04-01].

[12] VLK, Martin, Petra SUCHÁNKOVÁ and Ján KOZEMPEL. Medicinální radionuklidové generátory – mateřské radionuklidy, principy funkce a kontrola kvality eluátu. Nukleární Medicína. 2019, Vol. 8 (3.), str. 42 – 51. [cit. 2022-04-01].

[13] BOROS, Eszter, Cara L. FERREIRA, Jacqueline F. CAWTHRAY, Eric W. PRICE, Brian O. PATRICK, Dennis W. WESTER, Michael J. ADAM and Chris ORVIG. Acyclic Chelate with Ideal Properties for ^{68}Ga PET Imaging Agent Elaboration. *Journal of the American Chemical Society* [online]. 2010, **132**(44), 15726-15733 [cit. 2022-04-01]. ISSN 0002-7863. doi:10.1021/ja106399h

[14] NOTNI, Johannes and Hans-Jürgen WESTER. Re-thinking the role of radiometal isotopes: Towards a future concept for theranostic radiopharmaceuticals. *Journal of Labelled Compounds and Radiopharmaceuticals* [online]. 2018, **61**(3), 141-153 [cit. 2022-04-01]. ISSN 03624803. doi:10.1002/jlcr.3582

[15] ANDERSON, Carolyn J. and Michael J. WELCH. Radiometal-Labeled Agents (Non-Technetium) for Diagnostic Imaging. *Chemical Reviews* [online]. 1999, **99**(9), 2219-2234 [cit. 2022-04-01]. ISSN 0009-2665. doi:10.1021/cr980451q

[16] GREEN, Mark A. and Michael J. WELCH. Gallium radiopharmaceutical chemistry. *International Journal of Radiation Applications and Instrumentation. Part B. Nuclear Medicine and Biology* [online]. 1989, **16**(5), 435-448 [cit. 2022-04-01]. ISSN 08832897. doi:10.1016/0883-2897(89)90053-6

[17] BANDOLI, G, A DOLMELLA, F TISATO, M PORCHIA and F REFOSCO. Mononuclear six-coordinated Ga(III) complexes: A comprehensive survey. *Coordination Chemistry Reviews* [online]. 2009, **253**(1-2), 56-77 [cit. 2022-04-01]. ISSN 00108545. doi:10.1016/j.ccr.2007.12.001

[18] PRATA, I.M., 2012. Gallium-68: a new trend in PET radiopharmacy. Current radiopharmaceuticals, 5(2), pp.142-149. [cit. 2022-04-01].

[19] PEARSON, Ralph G. Hard and Soft Acids and Bases. Journal of the American Chemical Society [online]. 1963, 85(22), 3533-3539 [cit. 2022-04-01]. ISSN 0002-7863. doi:10.1021/ja00905a001

[20] HARRIS, Wesley R. and Vincent L. PECORARO. Thermodynamic binding constants for gallium transferrin. *Biochemistry* [online]. 1983, **22**(2), 292-299 [cit. 2022-04-01]. ISSN 0006-2960. doi:10.1021/bi00271a010

[21] IAEA Radioisotopes and Radiopharmaceuticals Series Publications: Production of Long Lived Parent Radionuclides for Generators: ^{68}Ge, ^{82}Sr, ^{90}Sr and ^{188}W. Vienna, Austria: International Atomic Energy Agency, 2010, 128 s. ISSN 2077-6462. Available at: http://www.iaea.org/Publications/index.html [cit. 2022-04-01].

[22] RÖSCH F.: ^{68}Ge/^{68}Ga Generators and ^{68}Ga Radiopharmaceutical Chemistry on Their Way into a New Century. J Postgrad Med Edu Res 2013;47(1):18-25. [cit. 2022-04-01].

[23] HENNRICH, Ute and Martina BENEŠOVÁ. [^{68}Ga]Ga-DOTA-TOC: The First FDA-Approved ^{68}Ga-Radiopharmaceutical for PET Imaging. *Pharmaceuticals* [online]. 2020, **13**(3) [cit. 2022-04-24]. ISSN 1424-8247. doi:10.3390/ph13030038

[24] COUNCIL OF EUROPE. (2019). European pharmacopoeia, 10th ed. Strasbourg, Council of Europe.

[25] MARUK, Alesya Ya. and Anton A. LARENKOV. Determination of ionic ^{68}Ga impurity in radiopharmaceuticals: major revision of radio-HPLC methods. *Journal of Radioanalytical and Nuclear Chemistry* [online]. 2020, **323**(1), 189-195 [cit. 2022-04-08]. ISSN 0236-5731. doi:10.1007/s10967-019-06964-1

[26] DE LEÓN-RODRÍGUEZ, Luis M. and Zoltan KOVACS. The Synthesis and Chelation Chemistry of DOTA−Peptide Conjugates. *Bioconjugate Chemistry* [online]. 2008, **19**(2), 391-402 [cit. 2022-04-02]. ISSN 1043-1802. doi:10.1021/bc700328s

[27] CORREIA, João D. G., António PAULO, Paula D. RAPOSINHO and Isabel SANTOS. Radiometallated peptides for molecular imaging and targeted therapy. *Dalton Transactions* [online]. 2011, **40**(23) [cit. 2022-04-03]. ISSN 1477-9226. doi:10.1039/c0dt01599g

[28] ROESCH, Frank and Patrick J. RISS. The Renaissance of the ^{68}Ge/^{68}Ga Radionuclide Generator Initiates New Developments in ^{68}Ga Radiopharmaceutical Chemistry. *Current Topics in Medicinal Chemistry* [online]. 2010, **10**(16), 1633-1668 [cit. 2022-04-06]. ISSN 15680266. doi:10.2174/156802610793176738

[29] SHI, Shengyu, Lifang ZHANG, Zehui WU, Aili ZHANG, Haiyan HONG, Seok Rye CHOI, Lin ZHU and Hank F. KUNG. [^{68}Ga]Ga-HBED-CC-DiAsp: A new renal function imaging agent. *Nuclear Medicine and Biology* [online]. 2020, **82-83**, 17-24 [cit. 2022-04-08]. ISSN 09698051. doi:10.1016/j.nucmedbio.2019.12.005

[30] TSIONOU, Maria Iris, Caroline E. KNAPP, Calum A. FOLEY, et al. Comparison of macrocyclic and acyclic chelators for gallium-68 radiolabelling. *RSC Adv* [online]. 2017, **7**(78), 49586-49599 [cit. 2022-04-03]. ISSN 2046-2069. doi:10.1039/C7RA09076E

[31] SPANG, Philipp, Christian HERRMANN and Frank ROESCH. Bifunctional Gallium-68 Chelators: Past, Present, and Future. *Seminars in Nuclear Medicine* [online]. 2016, **46**(5), 373-394 [cit. 2022-04-03]. ISSN 00012998. 10.1053/j.semnuclmed.2016.04.003

[32] BREEMAN, Wouter A. P., Marion DE JONG, Erik DE BLOIS, Bert F. BERNARD, Mark KONIJNENBERG and Eric P. KRENNING. Radiolabelling DOTA-peptides with ^{68}Ga. *European Journal of Nuclear Medicine and Molecular Imaging* [online]. 2005, **32**(4), 478-485 [cit. 2022-04-03]. ISSN 1619-7070. doi:10.1007/s00259-004-1702-y

[33] KOOP, Bernd, Sven N. RESKE and Bernd NEUMAIER. Labelling of a monoclonal antibody with ^{68}Ga using three DTPA-based bifunctional ligands and their *in vitro* evaluation for application in radioimmunotherapy. *Radiochimica Acta* [online]. 2007, **95**(1), 39-42 [cit. 2022-04-03]. ISSN 2193-3405. doi:10.1524/ract.2007.95.1.39

[34] KESSLER, R. M., J. C. GOBLE, J. H. BIRD, M. E. GIRTON, J. L. DOPPMAN, S. I. RAPOPORT a J. A. BARRANGER. Measurement of Blood—Brain Barrier Permeability with Positron Emission Tomography and [^{68}Ga]EDTA. *Journal of Cerebral Blood Flow & Metabolism* [online]. 1984, **4**(3), 323-328 [cit. 2022-04-06]. ISSN 0271-678X. doi:10.1038/jcbfm.1984.48

[35] WOOD, Scott A. and Iain M. SAMSON. The aqueous geochemistry of gallium, germanium, indium and scandium. *Ore Geology Reviews* [online]. 2006, **28**(1), 57-102 ISSN 01691368. doi:10.1016/j.oregeorev.2003.06.002 [cit. 2022 04-05].

[36] MCINNES, Lachlan E., Stacey E. RUDD and Paul S. DONNELLY. Copper, gallium and zirconium positron emission tomography imaging agents: The importance of metal ion speciation. *Coordination Chemistry Reviews* [online]. 2017, **352**, 499-516 [cit. 2022-04-05]. ISSN 00108545. doi:10.1016/j.ccr.2017.05.011

[37] PRICE, Eric W. and Chris ORVIG. Matching chelators to radiometals for radiopharmaceuticals. *Chem. Soc. Rev* [online]. 2014, **43**(1), 260-290 [cit. 2022-04-06]. ISSN 0306-0012. doi:10.1039/C3CS60304K

[38] JALILIAN, A.R., GAROSI, J., GHOLAMI, E., AKHLAGHI, M., SADDADI, F., BOLOURINOVIN, F. and KARIMIAN, A., 2007. Evaluation of [^{67}Ga]-insulin for insulin receptor imaging. *Nuclear Medicine Review*, 10(2), pp.71-75. [cit. 2022-04-08].

[39] BRECHBIEL, Martin W., Otto A. GANSOW, Robert W. ATCHER, Jeffrey SCHLOM, Jose ESTEBAN, Diane SIMPSON and David COLCHER. Synthesis of 1-(p-isothiocyanatobenzyl) derivatives of DTPA and EDTA. Antibody labeling and tumor-imaging studies. *Inorganic Chemistry* [online]. 1986, **25**(16), 2772-2781 [cit. 2022-04-08]. ISSN 0020-1669. doi:10.1021/ic00236a024

[40] MUYLLE, Kristoff, Patrick FLAMEN, Danielle J. VUGTS, et al. Tumour targeting and radiation dose of radioimmunotherapy with ^{90}Y-rituximab in CD20+ B-cell lymphoma as predicted by ^{89}Zr-rituximab immuno-PET: impact of preloading with unlabelled rituximab. *European Journal of Nuclear Medicine and Molecular Imaging* [online]. 2015, **42**(8), 1304-1314 [cit. 2022-04-10]. ISSN 1619-7070. doi:10.1007/s00259-015-3025-6

[41] KAPADIA, Nirav S., James M. ENGLES and Richard L. WAHL. *In Vitro* Evaluation of Radioprotective and Radiosensitizing Effects of Rituximab. *Journal of Nuclear Medicine* [online]. 2008, **49**(4), 674-678 [cit. 2022-04-10]. ISSN 0161-5505. doi:10.2967/jnumed.107.043752

[42] TENNVALL, Jan, Manfred FISCHER, Angelika BISCHOF DELALOYE, et al. EANM procedure guideline for radio-immunotherapy for B-cell lymphoma with ^{90}Y-radiolabelled ibritumomab tiuxetan (Zevalin). *European Journal of Nuclear Medicine and Molecular Imaging* [online]. 2007, **34**(4), 616-622 [cit. 2022-04-10]. ISSN 1619-7070. doi:10.1007/s00259-007-0372-y

[43] PANDEY, Usha, Mythili KAMESWARAN, Haladhar DEV SARMA and Grace SAMUEL. ^{99m}Tc carbonyl DTPA–Rituximab: Preparation and preliminary bioevaluation. *Applied Radiation and Isotopes* [online]. 2014, **86**, 52-56 [cit. 2022-04-10]. ISSN 09698043. doi:10.1016/j.apradiso.2013.12.036

[44] KEATING, Gillian M. Rituximab. *Drugs* [online]. 2010, **70**(11), 1445-1476 [cit. 2022-04-10]. ISSN 0012-6667. doi:10.2165/11201110-000000000-00000

[45] BOERMAN, Otto C. and Wim J.G. OYEN. Immuno-PET of Cancer: A Revival of Antibody Imaging. *Journal of Nuclear Medicine* [online]. 2011, **52**(8), 1171-1172 [cit. 2022-04-10]. ISSN 0161-5505. doi:10.2967/jnumed.111.089771

[46] NAHM, Daniel. Development of Biomaterial Inks for the Additive Manufacturing of Chemically Crosslinked Hydrogel Scaffolds: dissertation. Julius-Maximilians-Universität Würzbur, Würtzburg, 2020.

[47] SEDLÁČEK, Ondřej, Bryn D. MONNERY, Sergey K. FILIPPOV, Richard HOOGENBOOM and Martin HRUBÝ. Poly(2-Oxazoline)s - Are They More Advantageous for Biomedical Applications Than Other Polymers?. Macromolecular Rapid Communications [online]. 2012, 33(19), 1648-1662 [cit. 2022-03-19]. ISSN 10221336. doi:10.1002/marc.201200453

[48] LUXENHOFER, Robert, Yingchao HAN, Anita SCHULZ, Jing TONG, Zhijian HE, Alexander V. KABANOV and Rainer JORDAN. Poly(2-oxazoline)s as Polymer Therapeutics. Macromolecular Rapid Communications [online]. 2012, 33(19), 1613-1631 [cit. 2022-03-19]. ISSN 10221336. doi:10.1002/marc.201200354

[49] VERBRAEKEN, Bart, Bryn D. MONNERY, Kathleen LAVA and Richard HOOGENBOOM. The chemistry of poly(2-oxazoline)s. European Polymer Journal [online]. 2017, 88, 451-469 ISSN 00143057. doi:10.1016/j.eurpolymj.2016.11.016 [cit. 2022-03-19].

[50] BLOM, Elisabeth, Irina VELIKYAN, Azita MONAZZAM, et al. Synthesis and characterization of scVEGF-PEG-[^{68}Ga]NOTA and scVEGF-PEG-[^{68}Ga]DOTA PET tracers. *Journal of Labelled Compounds and Radiopharmaceuticals* [online]. 2011, **54**(11), 685-692 [cit. 2022-04-26]. ISSN 03624803. doi:10.1002/jlcr.1909

[51] JERCA, Valentin Victor, Kathleen LAVA, Bart VERBRAEKEN and Richard HOOGENBOOM. Poly(2-cycloalkyl-2-oxazoline)s: high melting temperature polymers solely based on Debye and Keesom van der Waals interactions. Polymer Chemistry [online]. 2016, 7(6), 1309-1322 [cit. 2022-03-21]. ISSN 1759-9954. doi:10.1039/C5PY01755F¨

[52] LAMBERMONT-THIJS, Hanneke M. L., Huub P. C. van KURINGEN, Jeroen P. W. van der PUT, Ulrich S. SCHUBERT and Richard HOOGENBOOM. Temperature Induced Solubility Transitions of Various Poly(2-oxazoline)s in Ethanol-Water Solvent Mixtures. Polymers [online]. 2010, 2(3), 188-199 [cit. 2022-03-23]. ISSN 2073-4360. doi:10.3390/polym2030188

[53] PIETSCH, Christian, Richard HOOGENBOOM and Ulrich S. SCHUBERT. Soluble Polymeric Dual Sensor for Temperature and pH Value. *Angewandte Chemie* [online]. 2009, **121**(31), 5763-5766 [cit. 2022-03-23]. ISSN 00448249. doi:10.1002/ange.200901071

[54] FRANK, Henry S. and Marjorie W. EVANS. Free Volume and Entropy in Condensed Systems III. Entropy in Binary Liquid Mixtures; Partial Molal Entropy in Dilute Solutions; Structure and Thermodynamics in Aqueous Electrolytes. *The Journal of Chemical Physics* [online]. 1945, **13**(11), 507-532 [cit. 2022-03-23]. ISSN 0021-9606. doi:10.1063/1.1723985

[55] FRANKS, F. and D. J. G. IVES. The structural properties of alcohol–water mixtures. *Q. Rev. Chem. Soc* [online]. 1966, **20**(1), 1-44 [cit. 2022-03-23]. ISSN 0009-2681. doi:10.1039/QR9662000001

[56] NOSKOV, Sergei Yu., Guillaume LAMOUREUX and Benoît ROUX. Molecular Dynamics Study of Hydration in Ethanol−Water Mixtures Using a Polarizable Force Field. *The Journal of Physical Chemistry B* [online]. 2005, **109**(14), 6705-6713 [cit. 2022-03-23]. ISSN 1520-6106. doi:10.1021/jp045438q

[57] LORSON, T., JAKSCH, S., LÜBTOW, M.M., JÜNGST, T., GROLL, J., LÜHMANN, T. and LUXENHOFER, R., 2017. A thermogelling supramolecular hydrogel with sponge-like morphology as a cytocompatible bioink. *Biomacromolecules*, *18*(7), pp.2161-2171. [cit. 2022-03-23].

[58] PAN, Xianfu, Yaya LIU, Zhenjiang LI, et al. Amphiphilic Polyoxazoline-block-Polypeptoid Copolymers by Sequential One-Pot Ring-Opening Polymerizations. *Macromolecular Chemistry and Physics* [online]. 2017, **218**(6) [cit. 2022-04-01]. ISSN 10221352. doi:10.1002/macp.201600483

[59] TAUHARDT, Lutz, David PRETZEL, Kristian KEMPE, Michael GOTTSCHALDT, Dirk POHLERS and Ulrich S. SCHUBERT. Zwitterionic poly(2-oxazoline)s as promising candidates for blood contacting applications. *Polym. Chem* [online]. 2014, **5**(19), 5751-5764 [cit. 2022-04-01]. ISSN 1759-9954. doi:10.1039/C4PY00434E

[60] SHAH, Rushita, Zuzana KRONEKOVA, Anna ZAHORANOVÁ, Ladislav ROLLER, Nabanita SAHA, Petr SAHA and Juraj KRONEK. In vitro study of partially hydrolyzed poly(2-ethyl-2-oxazolines) as materials for biomedical applications. *Journal of Materials Science: Materials in Medicine* [online]. 2015, **26**(4) [cit. 2022-04-01]. ISSN 0957-4530. doi:10.1007/s10856-015-5485-4

[61] VAN KURINGEN, Huub P. C., Joke LENOIR, Els ADRIAENS, Johan BENDER, Bruno G. DE GEEST and Richard HOOGENBOOM. Partial Hydrolysis of Poly(2-ethyl-2-oxazoline) and Potential Implications for Biomedical Applications? *Macromolecular Bioscience* [online]. 2012, **12**(8), 1114-1123 [cit. 2022-04-01]. ISSN 16165187doi:10.1002/mabi.201200080

[62] WYFFELS, Leonie, Thomas VERBRUGGHEN, Bryn D. MONNERY, Mathias GLASSNER, Sigrid STROOBANTS, Richard HOOGENBOOM and Steven STAELENS. μPET imaging of the pharmacokinetic behavior of medium and high molar mass ^{89}Zr-labeled poly(2-ethyl-2-oxazoline) in comparison to poly(ethylene glycol). *Journal of Controlled Release* [online]. 2016, **235**, 63-71 [cit. 2022-04-01]. ISSN 01683659. doi:10.1016/j.jconrel.2016.05.048

[63] ULBRICHT, Juliane, Rainer JORDAN and Robert LUXENHOFER. On the biodegradability of polyethylene glycol, polypeptoids and poly(2-oxazoline)s. *Biomaterials* [online]. 2014, **35**(17), 4848-4861 [cit. 2022-04-01]. ISSN 01429612. doi:10.1016/j.biomaterials.2014.02.029

[64] TANAKA, Ryuichi, Isao UEOKA, Yasuhiro TAKAKI, Kazuya KATAOKA and Shogo SAITO. High molecular weight linear polyethylenimine and poly(N-methylethylenimine). *Macromolecules* [online]. 1983, **16**(6), 849-853 [cit. 2022-04-01]. ISSN 0024-9297. doi:10.1021/ma00240a003

[65] TOMALIA, D. A. and D. P. SHEETZ. Homopolymerization of 2-alkyl- and 2-aryl-2-oxazolines. *Journal of Polymer Science Part A-1: Polymer Chemistry* [online]. **4**(9), 2253-2265 [cit. 2022-04-01]. ISSN 0449296X. doi:10.1002/pol.1966.150040919

[66] LAMBERMONT-THIJS, Hanneke M. L., Johan P. A. HEUTS, Stephanie HOEPPENER, Richard HOOGENBOOM and Ulrich S. SCHUBERT. Selective partial hydrolysis of amphiphilic copoly(2-oxazoline)s as basis for temperature and pH responsive micelles. *Polym. Chem* [online]. 2011, **2**(2), 313-322 [cit. 2022-04-01]. ISSN 1759-9954. doi:10.1039/C0PY00052C

[67] KEM, Kenneth M. Kinetics of the hydrolysis of linear poly[(acylimino)-ethylenes]. *Journal of Polymer Science: Polymer Chemistry Edition* [online]. **17**(7), 1977-1990 [cit. 2022-04-01]. ISSN 03606376. doi:10.1002/pol.1979.170170708

[68] LAMBERMONT-THIJS, Hanneke M. L., Friso S. VAN DER WOERDT, Anja BAUMGAERTEL, Lies BONAMI, Filip E. DU PREZ, Ulrich S. SCHUBERT and Richard HOOGENBOOM. Linear Poly(ethylene imine)s by Acidic Hydrolysis of Poly(2-oxazoline)s: Kinetic Screening, Thermal Properties, and Temperature-Induced Solubility Transitions. *Macromolecules* [online]. 2010, **43**(2), 927-933 [cit. 2022-04-01]. ISSN 0024-9297. doi:10.1021/ma9020455

[69] LAMBERMONT-THIJS, Hanneke M. L., Friso S. VAN DER WOERDT, Anja BAUMGAERTEL, Lies BONAMI, Filip E. DU PREZ, Ulrich S. SCHUBERT and Richard HOOGENBOOM. Linear Poly(ethylene imine)s by Acidic Hydrolysis of Poly(2-oxazoline)s: Kinetic Screening, Thermal Properties, and Temperature-Induced Solubility Transitions. *Macromolecules* [online]. 2010, **43**(2), 927-933 [cit. 2022-04-01]. ISSN 0024-9297. doi:10.1021/ma9020455

[70] NIMMO, Chelsea M. a Molly S. SHOICHET. Regenerative Biomaterials that "Click": Simple, Aqueous-Based Protocols for Hydrogel Synthesis, Surface Immobilization, and 3D Patterning. *Bioconjugate Chemistry* [online]. 2011, **22**(11), 2199-2209 [cit. 2022-04-01]. ISSN 1043-1802. doi:10.1021/bc200281k

[71] KOLB, H.C., FINN, M.G. and SHARPLESS, K.B., 2001. Click chemistry: diverse chemical function from a few good reactions. *Angewandte Chemie International Edition*, *40*(11), pp.2004-2021. [cit. 2022-04-01].

[72] CHUJO, Yoshiki, Kazuki SADA and Takeo SAEGUSA. Reversible gelation of polyoxazoline by means of Diels-Alder reaction. *Macromolecules* [online]. 1990, **23**(10), 2636-2641 ISSN 0024-9297. doi:10.1021/ma00212a007 [cit. 2022-04-01].

[73] LALLANA, Enrique, Ana SOUSA-HERVES, Francisco FERNANDEZ-TRILLO, Ricardo RIGUERA and Eduardo FERNANDEZ-MEGIA. Click Chemistry for Drug Delivery Nanosystems. *Pharmaceutical Research* [online]. 2012, **29**(1), 1-34 [cit. 2022-04-01]. ISSN 0724-8741. doi:10.1007/s11095-011-0568-5

[74] KIRCHHOF, Susanne, Ferdinand P. BRANDL, Nadine HAMMER and Achim M. GOEPFERICH. Investigation of the Diels–Alder reaction as a cross-linking mechanism for degradable poly(ethylene glycol) based hydrogels. *Journal of Materials Chemistry B* [online]. 2013, **1**(37) [cit. 2022-04-01]. ISSN 2050-750X. doi:10.1039/c3tb20831a

[75] KIRCHHOF, Susanne, Manuel GREGORITZA, Viktoria MESSMANN, Nadine HAMMER, Achim M. GOEPFERICH and Ferdinand P. BRANDL. Diels-Alder hydrogels with enhanced stability: First step toward controlled release of bevacizumab. *European Journal of Pharmaceutics and Biopharmaceutics* [online]. 2015, **96**, 217-225 [cit. 2022-04-01]. ISSN 09396411. doi:10.1016/j.ejpb.2015.07.024

[76] HEIN, Christopher D., Xin-Ming LIU and Dong WANG. Click Chemistry, A Powerful Tool for Pharmaceutical Sciences. *Pharmaceutical Research* [online]. 2008, **25**(10), 2216-2230 ISSN 0724-8741. doi:10.1007/s11095-008-9616-1 [cit. 2022-04-01].

[77] GREGORITZA, Manuel and Ferdinand P. BRANDL. The Diels–Alder reaction: A powerful tool for the design of drug delivery systems and biomaterials. *European Journal of Pharmaceutics and Biopharmaceutics* [online]. 2015, **97**, 438-453 [cit. 2022-04-01]. ISSN 09396411. doi:10.1016/j.ejpb.2015.06.007

[78] DIELS, Otto and Kurt ALDER. Synthesen in der hydroaromatischen Reihe. *Justus Liebig's Annalen der Chemie* [online]. 1928, **460**(1), 98-122 [cit. 2022-04-01]. ISSN 00754617. doi:10.1002/jlac.19284600106

[79] LALLANA, Enrique, Ana SOUSA-HERVES, Francisco FERNANDEZ-TRILLO, Ricardo RIGUERA and Eduardo FERNANDEZ-MEGIA. Click Chemistry for Drug Delivery Nanosystems. *Pharmaceutical Research* [online]. 2012, **29**(1), 1-34 [cit. 2022-04-01]. ISSN 0724-8741. doi:10.1007/s11095-011-0568-5

[80] CHUJO, Yoshiki, Kazuki SADA, Akio NAKA, Ryoji NOMURA and Takeo SAEGUSA. Synthesis and redox gelation of disulfide-modified polyoxazoline. *Macromolecules* [online]. 1993, **26**(5), 883-887 [cit. 2022-04-01]. ISSN 0024-9297. doi:10.1021/ma00057a001

[81] CHUJO, Yoshiki, Kazuki SADA and Takeo SAEGUSA. Iron(II) bipyridyl-branched polyoxazoline complex as a thermally reversible hydrogel. *Macromolecules* [online]. 1993, **26**(24), 6315-6319 [cit. 2022-04-01]. ISSN 0024-9297.10.1021/ma00076a001

[82] CHUJO, Yoshiki, Kazuki SADA a Takeo SAEGUSA. Cobalt(III) bipyridyl branched polyoxazoline complex as a thermally and redox reversible hydrogel. *Macromolecules* [online]. 1993, **26**(24), 6320-6323 [cit. 2022-04-01]. ISSN 0024-9297. Dostupné z: doi:10.1021/ma00076a002

[83] NICOLAOU, K.C., SNYDER, S.A., MONTAGNON, T. and VASSILIKOGIANNAKIS, G., 2002. The Diels–Alder reaction in total synthesis. *Angewandte Chemie International Edition*, *41*(10), pp.1668-1698. [cit. 2022-04-01].

[84] TANG, Shi-Ya, Jing SHI and Qing-Xiang GUO. Accurate prediction of rate constants of Diels–Alder reactions and application to design of Diels–Alder ligation. *Organic & Biomolecular Chemistry* [online]. 2012, **10**(13) [cit. 2022-04-01]. ISSN 1477-0520. doi:10.1039/c2ob07079

[85] LINDSTRÖM, Ulf M. Stereoselective Organic Reactions in Water. *Chemical Reviews* [online]. 2002, **102**(8), 2751-2772 [cit. 2022-04-01]. ISSN 0009-2665. doi:10.1021/cr010122p

[86] TTO, S. and ENGBERTS, J.B., 2000. Special Topic Issue on Green Chemistry. *Pure Appl. Chem*, *72*(7), pp.1365-1372. [cit. 2022-04-01].

[87] PALOMO, Jose M. Diels–Alder Cycloaddition in Protein Chemistry. *European Journal of Organic Chemistry* [online]. 2010, **2010**(33), 6303-6314 [cit. 2022-04-01]. ISSN 1434-193X. doi:10.1002/ejoc.201000859

[88] WOODWARD, R.B. and Thomas J. KATZ. The mechanism of the Diels-Alder reaction. *Tetrahedron* [online]. 1959, **5**(1), 70-89 [cit. 2022-04-01]. ISSN 00404020. doi:10.1016/0040-4020(59)80072-7

[89] SAUER, Jürgen and Reiner SUSTMANN. Mechanistic Aspects of Diels-Alder Reactions: A Critical Survey. *Angewandte Chemie International Edition in English* [online]. 1980, **19**(10), 779-807 [cit. 2022-04-01]. ISSN 0570-0833. doi:10.1002/anie.198007791

[90] KUMAMOTO, Koji, Isao FUKADA and Hiyoshizo KOTSUKI. Diels–Alder Reaction of Thiophene: Dramatic Effects of High-Pressure/Solvent-Free Conditions. *Angewandte Chemie International Edition* [online]. 2004, **43**(15), 2015-2017 [cit. 2022-04-01]. ISSN 1433-7851. doi:10.1002/anie.200353487

[91] GANDINI, Alessandro. The furan/maleimide Diels–Alder reaction: A versatile click–unclick tool in macromolecular synthesis. *Progress in Polymer Science* [online]. 2013, **38**(1), 1-29 ISSN 00796700. doi:10.1016/j.progpolymsci.2012.04.002 [cit. 2022-04-01].

[92] BRESLOW, Ronald, Uday MAITRA and Darryl RIDEOUT. Selective Diels-Alder reactions in aqueous solutions and suspensions. *Tetrahedron Letters* [online]. 1983, **24**(18), 1901-1904 [cit. 2022-04-01]. ISSN 00404039. doi:10.1016/S0040-4039(00)81801-8

[93] FERNANDEZ, C A, N J BAUMHOVER, J T DUSKEY, S KHARGHARIA, K KIZZIRE, M D ERICSON and K G RICE. Metabolically stabilized long-circulating PEGylated polyacridine peptide polyplexes mediate hydrodynamically stimulated gene expression in liver. *Gene Therapy* [online]. 2011, **18**(1), 23-37 [cit. 2022-04-01]. ISSN 0969-7128. doi:10.1038/gt.2010.117

[94] KIRCHHOF, Susanne, Manuel GREGORITZA, Viktoria MESSMANN, Nadine HAMMER, Achim M. GOEPFERICH and Ferdinand P. BRANDL. Diels-Alder hydrogels with enhanced stability: First step toward controlled release of bevacizumab. *European Journal of Pharmaceutics and Biopharmaceutics* [online]. 2015, **96**, 217-225 [cit. 2022-04-01]. ISSN 09396411. doi:10.1016/j.ejpb.2015.07.024

[95] YANG, Kejia, Jesse C. GRANT, Patrice LAMEY, Alexandra JOSHI-IMRE, Benjamin R. LUND, Ronald A. SMALDONE and Walter VOIT. Diels–Alder Reversible Thermoset 3D Printing: Isotropic Thermoset Polymers via Fused Filament Fabrication. *Advanced Functional Materials* [online]. 2017, **27**(24) [cit. 2022-04-01]. ISSN 1616-301X. doi:10.1002/adfm.201700318

[96] CHEN, Xiangxu, Matheus A. DAM, Kanji ONO, Ajit MAL, Hongbin SHEN, Steven R. NUTT, Kevin SHERAN and Fred WUDL. A Thermally Re-mendable Cross-Linked Polymeric Material. *Science* [online]. 2002, **295**(5560), 1698-1702 [cit. 2022-04-01]. ISSN 0036-8075. 10.1126/science.1065879

[97] Encyclopedia of Polymer Science and Technology - Plastics, Resins, Rubbers, Fibers. Vol. 5: Dielectric Heating to Emulsion. Vol. 6. *Chemie Ingenieur Technik - CIT* [online]. 1969, **41**(10), 637-637 [cit. 2022-04-01]. ISSN 0009-286X. doi:10.1002/cite.330411014

[98] LIU, Ying-Ling and Tsai-Wei CHUO. Self-healing polymers based on thermally reversible Diels–Alder chemistry. *Polymer Chemistry* [online]. 2013, **4**(7) [cit. 2022-04-01]. ISSN 1759-9954.10.1039/c2py20957h

[99] SHI, Meng and Molly S. SHOICHET. Furan-functionalized co-polymers for targeted drug delivery: caracterization, self-assembly and drug encapsulation. *Journal of Biomaterials Science, Polymer Edition* [online]. 2012, **19**(9), 1143-1157 [cit. 2022-04-01]. ISSN 0920-5063. doi:10.1163/156856208785540127

[100] DREISS, Cécile A. Hydrogel design strategies for drug delivery. *Current Opinion in Colloid & Interface Science* [online]. 2020, **48**, 1-17 [cit. 2022-04-11]. ISSN 13590294. doi:10.1016/j.cocis.2020.02.001

[101] THAMBI, Thavasyappan, Yi LI and Doo Sung LEE. Injectable hydrogels for sustained release of therapeutic agents. *Journal of Controlled Release* [online]. 2017, **267**, 57-66 ISSN 01683659. doi:10.1016/j.jconrel.2017.08.006 [cit. 2022-04-11].

[102] LUXENHOFER, Robert, Yingchao HAN, Anita SCHULZ, Jing TONG, Zhijian HE, Alexander V. KABANOV and Rainer JORDAN. Poly(2-oxazoline)s as Polymer Therapeutics. *Macromolecular Rapid Communications* [online]. 2012, **33**(19), 1613-1631 ISSN 10221336. doi:10.1002/marc.201200354 [cit. 2022-04-11].

[103] LI, Jianyu and David J. MOONEY. Designing hydrogels for controlled drug delivery. *Nature Reviews Materials* [online]. 2016, **1**(12) [cit. 2022-04-11]. ISSN 2058-8437. doi:10.1038/natrevmats.2016.71

[104] HRUBÝ, Martin, Sergey K. FILIPPOV and Petr ŠTĚPÁNEK. Smart polymers in drug delivery systems on crossroads: Which way deserves following?. *European Polymer Journal* [online]. 2015, **65**, 82-97 [cit. 2022-04-11]. ISSN 00143057. doi:10.1016/j.eurpolymj.2015.01.016

[105] KRIZMAN, P., CERNELIC, K., WONDRA, A., RODIC, Z. and PROSEK, M., 2013. The importance of standardization in quantitative thin-layer chromatography—retrospective and case studies. *JPC-Journal of Planar Chromatography-Modern TLC*, *26*(4), pp.299-305. [cit. 2022-04-11].